Geoscience Frontiers 14 (2023) 101628

Contents lists available at ScienceDirect

Geoscience Frontiers

journal homepage: www.elsevier.com/locate/gsf

Research Paper

Control of inherited structural fabric on the development and exhumation of passive margins – Insights from the Araçuaí Orogen (Brazil)

Ana Fonseca [a,*], Tiago Novo [b,c], Tobias Fonte-Boa [b,c], Matheus Kuchenbecker [c,d], Daniel Galvão Carnier Fragoso [e,f], Daniel Peifer [g], Antônio Carlos Pedrosa-Soares [b,c], Johan De Grave [a]

[a] Laboratory for Mineralogy and Petrology, Department of Geology, Ghent University, Krijgslaan 281 S8, 9000 Ghent, Belgium
[b] Universidade Federal de Minas Gerais, Programa de Pós-Graduação em Geologia, CPMTC-IGC, Campus Pampulha, Belo Horizonte, MG, Brazil
[c] Centro de Pesquisas Professor Manoel Teixeira da Costa, Instituto de Geociências, Universidade Federal de Minas Gerais, Belo Horizonte, Brazil
[d] Universidade Federal dos Vales do Jequitinhonha e Mucuri, Instituto de Ciência e Tecnologia, Centro de Estudos em Geociências, Laboratório de Estudos Tectônicos, Diamantina, Brazil
[e] Petrobras, Rio de Janeiro, RJ, Brazil
[f] Instituto de Geociências, Universidade Federal do Rio Grande do Sul, Porto Alegre, RS, Brazil
[g] Department of Geosciences, University of Tübingen, Schnarrenbergstr. 94-96, 72076 Tübingen, Germany

ARTICLE INFO

Article history:
Received 18 January 2023
Revised 23 March 2023
Accepted 28 April 2023
Available online 6 May 2023
Handling Editor: Sanghoon Kwon

Keywords:
Thermal history
Denudation
Tectonic inheritance
Reactivations
South Atlantic
Hydrocarbons

ABSTRACT

The Araçuaí Orogen, in eastern Brazil, was formed during the Neoproterozoic – Cambrian amalgamation of West Gondwana. During the Mesozoic – Cenozoic opening of the South Atlantic Ocean, and the associated divergent tectonics, the orogen developed as basement to the passive margin of South America and was progressively covered by thick offshore sedimentary basins, particularly the Espírito Santo, Mucuri, and Cumuruxatiba basins, in which hydrocarbon systems have been exploited. Our understanding of the Araçuaí Orogen's passive margin evolution, erosion, and sediment transfer to these basins ultimately depends on constraining the onshore exhumation in response to Mesozoic – Cenozoic events. Here, new and previously published data from apatite fission-track (AFT) analyses and inverse thermal history modelling of (Pre)Cambrian basement rocks from the Araçuaí Orogen resolve three discrete basement cooling and associated erosional exhumation episodes. In the Pre-Rift phase, Jurassic – Hauterivian erosion of the Araçuaí Orogen is most likely related to the adjoining intra-continental West Gondwana flexural subsidence, which increased hillslope and river erosion power. In the Rift and Transitional phases, Barremian – Albian accelerated phase of erosion is associated with the uplift of the Atlantic rift shoulders and the establishment of an oceanic base-level. In the Drift phase, reactivations in response to far-field stresses likely triggered a Late Cretaceous – Paleocene rapid erosion event. The rates at which these events unfolded vary spatially and are controlled by inherited structures. The Araçuaí Orogen experienced slower denudation rates in areas closer to the São Francisco Craton, which suggests that the tectonic reactivation and related surface uplift during the Mesozoic–Cenozoic is in first-order controlled by lithospheric rigidity. Furthermore, the structural framework of the Paramirim and Pirapora aulacogens and NE-oriented shear zones in the orogen's southeast facilitated later reactivations. From the spatial pattern of denudation/exhumation of the Araçuaí Orogen during the Mesozoic – Cenozoic, we draw inferences on the tectonic development of the offshore basins regarding their hydrocarbon potentials.

1. Introduction

The Araçuaí Orogen is the South American section of a larger Neoproterozoic – Cambrian orogenic system, i.e. the Araçuaí-West Congo Orogen (AWCO) (Fig. 1; Pedrosa-Soares et al., 2008). In the Late Jurassic – Early Cretaceous, the Araçuaí Orogen separated from its African counterpart during the process of the Gondwana breakup and the subsequent opening of the South Atlantic Ocean (Torsvik et al., 2009; Mohriak and Fainstein, 2012). At that time, the extensional deformation reactivated crustal heterogeneities produced by earlier orogenic processes, and these reacti-

* Corresponding author.
E-mail address: anacarolina.LiberalFonseca@ugent.be (A. Fonseca).

https://doi.org/10.1016/j.gsf.2023.101628

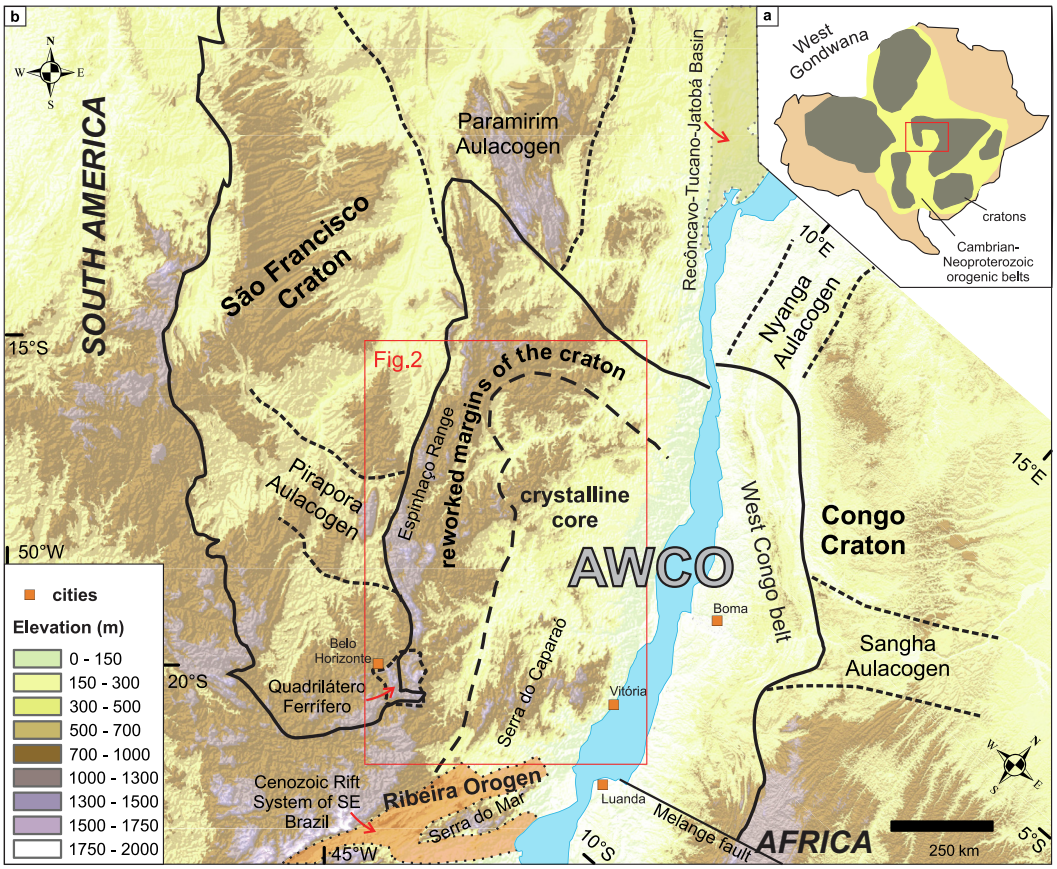

Fig. 1. Geological context of the study area. (a) Schematic representation of West Gondwana with its cratonic continental cores and Neoproterozoic–Cambrian orogenic belts (after Tohver et al., 2006; Vaughan and Pankhurst, 2008). (b) Elevation map showing a reconstruction of the São Francisco and Congo cratons and the Araçuaí–West Congo Orogen (AWCO), with the main tectonic and morphological units. Topographic data: Copernicus (COP30) digital elevation model (DEM) with a spatial resolution of 30 m.

vated structures functioned as mechanical discontinuities along thrust detachments (Ashby et al., 2010; Nemčok, 2016; Salomon et al., 2017; Reuber and Mann, 2019). In addition to the Atlantic rifting, intraplate stresses during the Cenozoic resulted in significant intracontinental deformation and magmatism. Examples include volcanic features in several offshore basins (e.g., Abrolhos magmatism) and igneous plugs in adjacent onshore regions (Santiago et al., 2020; Stanton et al., 2022). Despite occurring about 300 Ma prior to the orogeny, we know substantially less about the Mesozoic – Cenozoic exhumation of the Araçuaí Orogen as a passive margin than about the orogeny itself.

Deciphering the timing and patterns of passive margin tectonics and intracontinental reactivation are essential for resolving the Mesozoic – Cenozoic evolution and its driving mechanisms in the Araçuaí Orogen region. However, because, for example, surface uplift is challenging to discern directly from the continental rock record, there remains discussion on how extensive surface uplift was during syn-/post-rifting phases and how this was expressed in the geomorphology (e.g., Stanley et al., 2021). Typically, surface uplift is inferred from erosion that may be traced from the detrital sedimentary record (e.g., Modica and Brush, 2004; Zalán et al., 2005; Mohriak et al., 2008; Contreras et al., 2010). In addition, constraining the magnitude and timing of onshore denudation is a crucial component of understanding erosion and sediment transfer across continental margins. Apatite fission-track (AFT) thermochronometry has been successfully used to estimate exhumation and burial along continental margins (see Wildman et al. 2019 for a review), providing valuable data on the timing and magnitude of rock cooling. AFT data can be used to reconstruct thermal histories using numerical modeling software in a low-temperature (i.e., shallow crustal) range (<120 °C; e.g., Gallagher, 2012). Therefore, AFT thermochronology has become a powerful tool for evaluating geological processes in the upper crust, such as tectonic processes exhuming deeper crustal roots, deep sedimentary or tectonic burial, and processes affecting landscape evolution (Flament et al., 2013).

While the southern and western parts of the Araçuaí Orogen have been explored using AFT to some extent (Carmo, 2005; Jelinek et al., 2014; Amaral-Santos et al., 2019; Van Ranst et al., 2020a; Fonseca et al., 2021), there are few to no constraints on the thermal history of the rocks in the northern and northeastern parts of the orogen (Fig. 2). In this contribution, we reconstruct the thermo-tectonic of the upper crust of the Araçuaí Orogen since its Mesozoic break-up on the basis of integrating new and published thermochronological data. The new data and thermal history models presented here considerably augment the available data set, allowing us to establish a more comprehensive understanding of exhumation and erosion along the eastern margin of the South Atlantic Ocean. Furthermore, we leverage the AFT data to obtain thermal history models and to constrain the temporal and spatial basement exhumation patterns, thereby clarifying the timing and driving mechanisms of Mesozoic – Cenozoic reactivations.

We emphasize that our study gives insights into the impact of the onshore exhumation on the development of the adjoining passive margin basins, some of which contain significant hydrocarbon potential. The Atlantic offshore area of the Araçuaí Orogen is covered by three main and adjacent basins, referred to as the Espírito

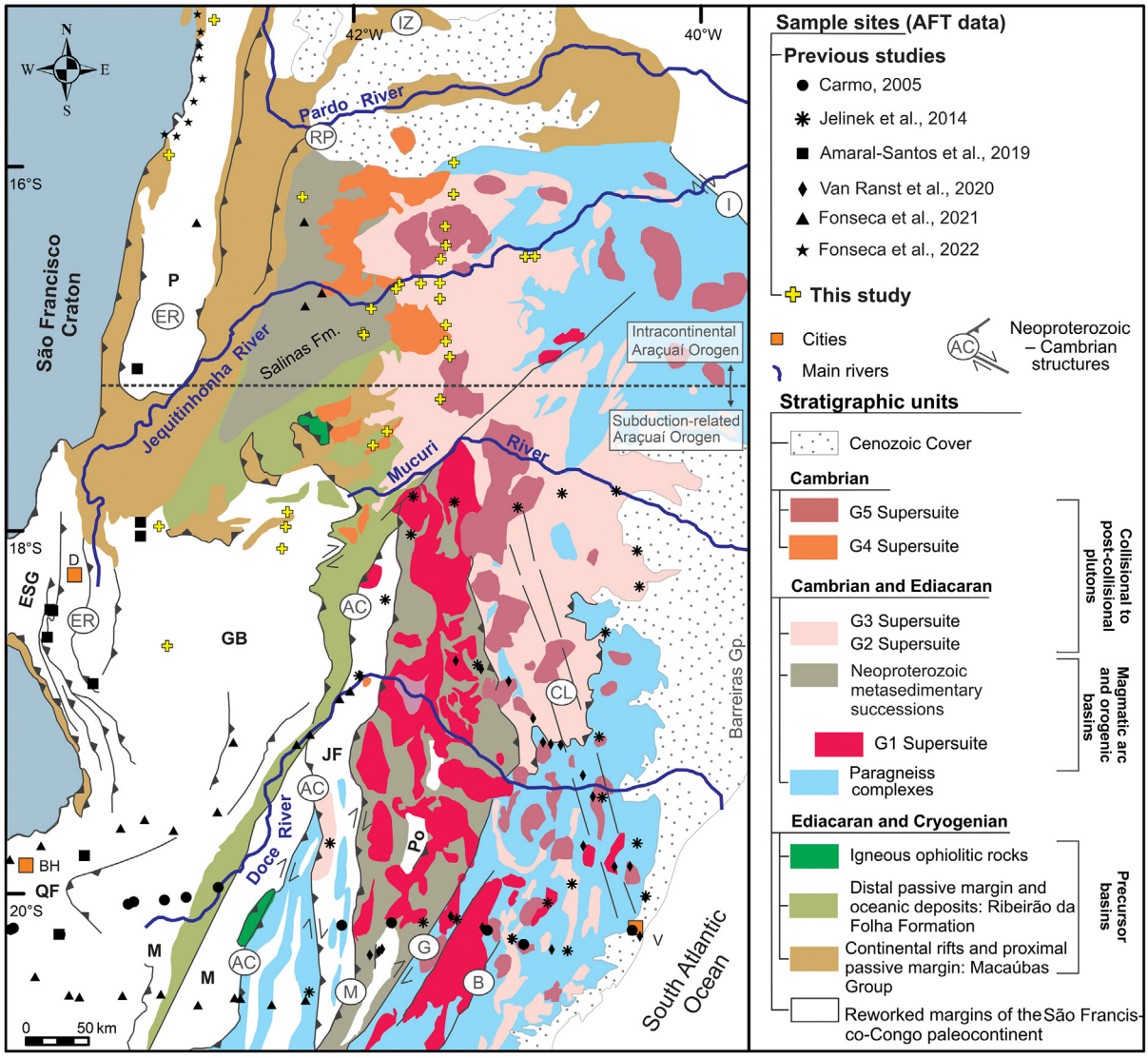

Fig. 2. Simplified geological map of the Araçuaí Orogen (after Pedrosa-Soares et al., 2007) with the sample site locations of new (this study) and published AFT data (Carmo, 2005; Jelinek et al., 2014; Amaral-Santos et al., 2019; Van Ranst et al., 2020a; Fonseca et al., 2021, 2022). Precambrian units: ESG–Espinhaço Supergroup; GB–Guanhães Block; QF–Quadrilátero Ferrífero; and JF–Juiz de Fora, M–Mantiqueira, P–Porterinha, and Po–Pocrane complexes. Tectonic domains: ER–Espinhaço Range, IZ–interaction zone with the Paramirim Aulacogen, RP–Rio Pardo salient, and AC–Abre Campo, B–Batatal, CL – Vitoria-Colatina, G–Guaçuí, I–Itapebi, and M–Manhuaçu shear zones. Major cities: BH–Belo Horizonte, V– Vitória, D–Diamantina.

Santo, Mucuri and Cumuruxatiba basins, from south to north (Figs. 3 and 4). In these basins, the entire sedimentary record associated with the opening of the Atlantic is preserved from its early phase in the Late Jurassic, with continental deposition in the Afro-Brazilian depression, through the present period of marine sedimentation along the passive margin. This evolutionary story can be told from the perspective of source area denudation. Exhumation patterns established from thermochronometry data and thermal history models illuminate how the denudation of the Araçuaí Orogen controlled sedimentary input into these basins, and how other processes such as halokinesis affected these basins.

2. Geological setting

The Araçuaí–West Congo Orogen (AWCO) was formed during the Ediacaran – Early Paleozoic amalgamation of West Gondwana as the consequence of the closure of a confined ocean branch within a gulf of the São Francisco-Congo paleocontinent (Pedrosa-Soares et al., 2001, 2008, 2020; Alkmim et al., 2006, 2017; Caxito et al., 2022). The São Francisco (South America) and Congo (Africa) cratons are the remnants of this ancient continent, and delineate the AWCO on its eastern, western and northern sides (Fig. 1). In Brazil, the AWCO's southern boundary has been arbitrarily set around latitude 21° S (Pedrosa-Soares et al., 2001) where the orogenic system continues to the south as the Ribeira Orogen (Fig. 1; Heilbron et al., 2000; Alkmim et al., 2017; Degler et al., 2017). The AWCO region remained a single and unified block until the Late Jurassic – Early Cretaceous, when it was broken into two pieces during opening of the South Atlantic Ocean: the Araçuaí Orogen (South America) and West-Congo Belt (Africa) (Fig. 1, Pedrosa-Soares et al., 2001, 2008; Tack et al., 2001; Alkmim et al., 2006). Since this extensional event, the rocks of the Araçuaí Orogen became the basement of rift to passive margin basins formed on the Brazilian Atlantic coast, whose successions host important sources and reservoirs of hydrocarbon systems (e.g., Mohriak and Fainstein, 2012). In the following section, we overview the (Pre)Cambrian units of the Araçuaí Orogen and the geology of the adjoining Mesozoic – Cenozoic coastal basins.

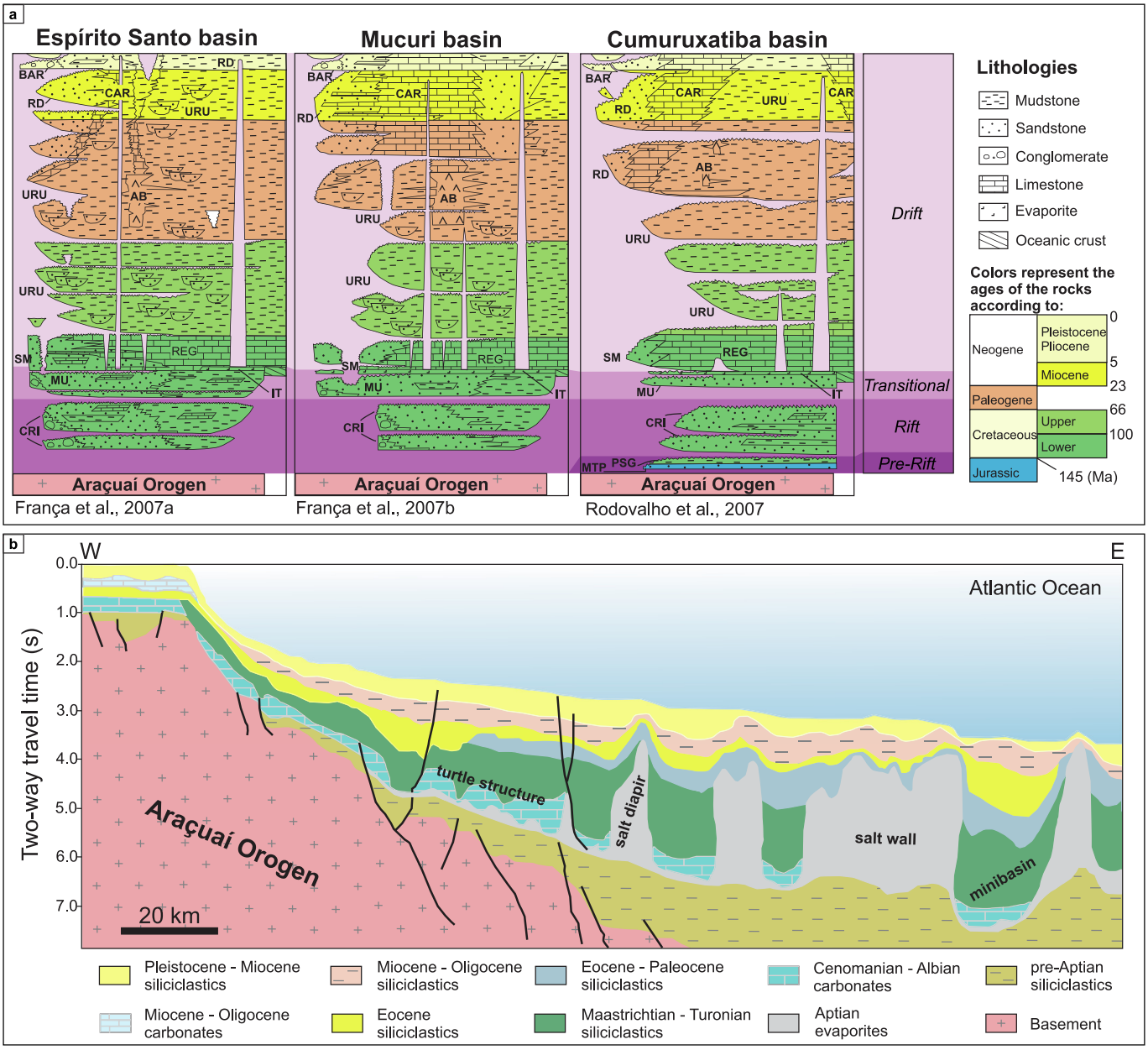

Fig. 3. (a) Schematic stratigraphic column of the Espírito Santo, Mucuri, and Cumuruxatiba basins (for locations see Fig. 4). Units: MTP – Monte Pascoal, PSG– Porto Seguro, CRI – Cricaré, MU – Mucuri, IT – Itaúnas, SM – São Mateus, REG – Regência, URU – Urucutuca, RD – Rio Doce, and CAR – Caravelas Formations, BAR – Barreiras Group, AB – Abrolhos magmatic rocks. (b) Schematic seismic section through the Espírito Santo Basin with halokinetic structures (after Mohriak et al., 2012).

2.1. Geology of the Araçuaí Orogen

The Araçuaí Orogen comprises two main domains: (i) an external fold-and-thrust belt, along its curved boundary with the São Francisco craton, and (ii) a crystalline metamorphic/anatetic core, which dominate its eastern portion and make the Brazilian Atlantic coast between the parallels 16° and 21° (Fig. 1). The external fold-and-thrust belt is characterized by the presence of basement inliers, pieces of the São Francisco-Congo paleocontinent margin that were involved in the deformation. These domains, such as the Guanhães, Mantiqueira, Juiz de Fora and Quadrilátero Ferrífero, encompasses Archean and Paleoproterozoic (>1.8 Ga) crystalline and supracrustal rocks whose origin trace back to the Rhyacian-Orosirian Minas Bahia orogeny, in which the paleocontinent was formed (e.g. Noce et al., 2007; Degler et al., 2017, 2018; Grochowski et al., 2021). These basement inliers are tectonically surrounded by supracrustal (and associated anorogenic igneous) rocks formed in the various extensional cycles that affected the São Francisco-Congo paleocontinent between the Statherian and the Cryogenian (e.g. Pedrosa-Soares et al., 2011; Guadagnin et al., 2015), and by rocks formed during the orogenesis. In this context, the rocks of the Espinhaço Supergroup (Statherian-Stenian; Chemale et al., 2012; Santos et al., 2015; Costa et al., 2018a, 2018b), Macaúbas Group (Tonian-Cryogenian; Pedrosa-Soares et al., 2011; Babinski et al., 2012; Kuchenbecker et al., 2015; Vilela et al., 2021) and Salinas Formation (Ediacaran-Cambrian; Santos et al., 2009; Kuchenbecker et al., 2020) deserve special mention. Important points to highlight are: (i) the successive rifting events occurred in the São Francisco-Congo paleocontinent during the Paleoproterozoic-Neoproterozoic have formed an intricated system of aulacogens, most of these aulacogens was reworked within the Neoproterozoic orogens, but some branches remain pre-

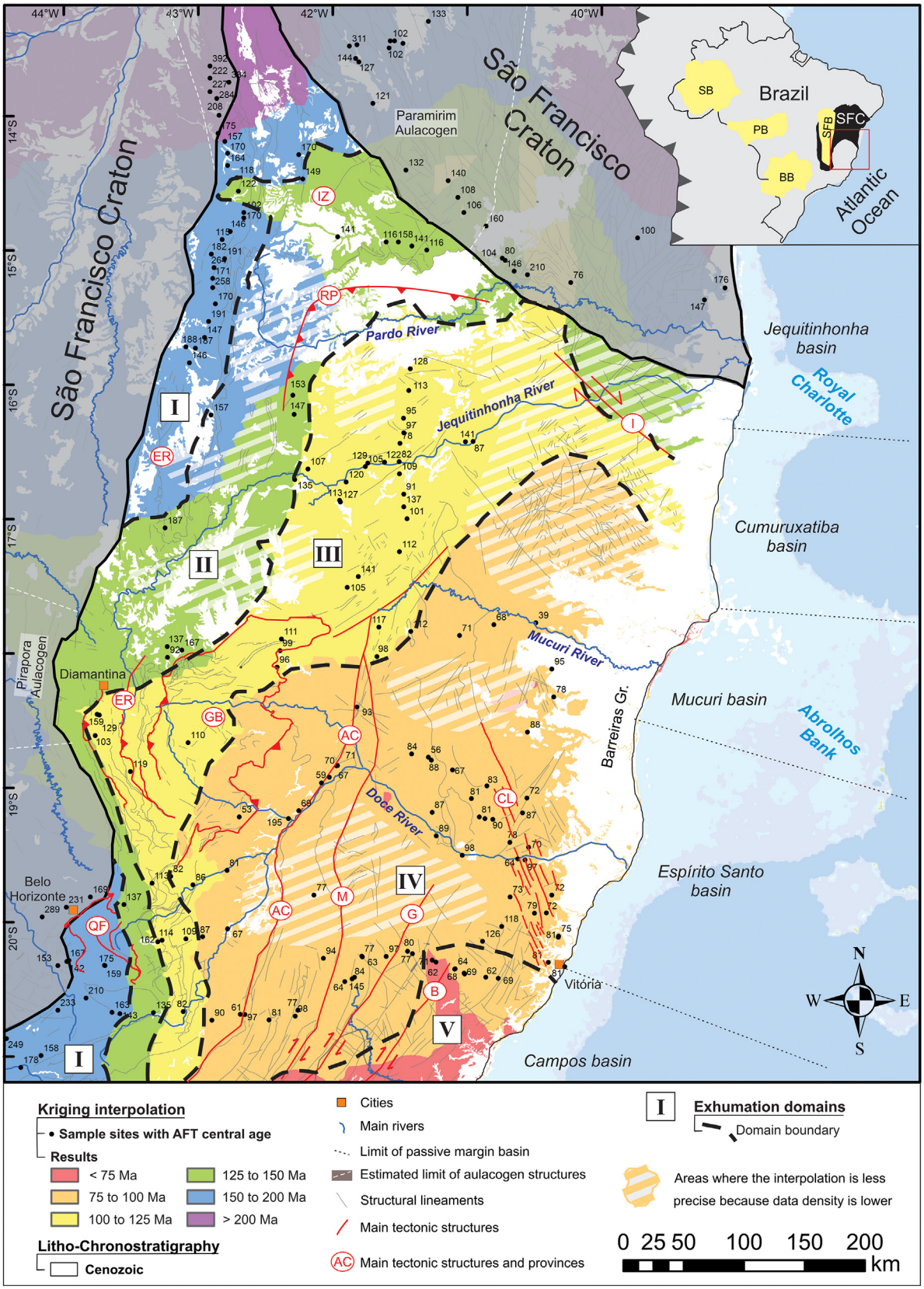

Fig. 4. Apatite Fission Track (AFT) central age and interpolated map of AFT ages obtained from new and published data. BB: Bauru, PB: Parecis, SFB: Sanfranciscana, and SB: Solimões basins. See text for further discussion.

served within the cratons, like the Pirapora and Paramirim (SFC) and Sangha (CC) aulacogens (Fig. 1; Cruz et al., 2015; Reis et al., 2017); (ii) the middle and upper units of the Macaúbas Group register the rift to passive margin deposits formed during the opening of the gulf that precedes the Araçuaí Orogen (Kuchenbecker et al., 2015; Amaral et al., 2020; Pedrosa-Soares et al., 2020).

The crystalline core of the Araçuaí Orogen encompasses Neoproterozoic ophiolite slivers, the magmatic arc system, and *syn*-collisional to post-collisional magmatic complexes (Fig. 2; Pedrosa-Soares et al., 2008, 2020). The tectonic evolution of the Araçuaí Orogen consists of four stages, with five different periods/types of magma production (from G1 to G5). These are: (i) pre-collisional (630 – 585 Ma) calc-alkaline I-type G1 supersuite; (ii) *syn*-collisional (585 – 540 Ma) S-type G2 supersuite; (iii) late-collisional (530 – 500 Ma) G3 supersuite, related to lateral tectonic escape with the formation of large shear zones; and (iv) post-collisional stages (525 – 490 Ma) that developed during the gravitational collapse of the orogen and resulted in the emplacement of the G4 and G5 supersuites (Fig. 2; for more details regarding the supersuites, see Pedrosa-Soares et al., 2011, 2020).

2.2. Structural framework and metamorphism

From a tectonic and metamorphic point of view, the Araçuaí Orogen can be subdivided into two major domains: the external low- to medium-grade fold-and-thrust belt and the internal high-grade granitic orogenic core (Fig. 1). These domains are separated by the dextral Abre Campo shear zone, a major structural and geophysical discontinuity in the orogen extending for >300 km. The Abre Campo shear zone is commonly interpreted as the suture zone of the AWCO (Fig. 2; e.g., Peixoto et al., 2015).

The fold-and-thrust belt extends from the edge of the SFC to the eastern border of the Guanhães block in the Abre Campo shear zone (Fig. 2). West-verging thrusts and associated folds are the main structural elements of its central sector. In contrast, NS to NE-trending dextral strike-slip shear zones dominate the structural fabric of the southern segment (Alkmim et al., 2017). Bordering the SFC, the Espinhaço Range exhibits an array of N–S structures that involve the basement, the Espinhaço Supergroup, and the Macaúbas Group (Dussin and Dussin, 1995; Pedrosa-Soares et al., 2011). The structural characteristics of the southern segment of the Espinhaço Range describe a relatively smooth salient that coincides with the presence of the WNW-trending Pirapora aulacogen (Fig. 1; Reis et al., 2017). To the north, these structures bend to the NNE and continue in this direction, forming the western edge of the interaction zone with the Paramirim aulacogen (Fig. 2; Cruz and Alkmim, 2006, 2017). Thereafter, the fold-and-thrust belt curves progressively towards the northeast to form the Rio Pardo salient (Peixoto et al., 2018). Greenschist assemblages predominate in the western section of the fold-and-thrust belt, close to the craton, whereas amphibolite facies rocks occur predominantly more to the east and in the more internal domains (e.g., Peixoto et al., 2018). In the northern segment of the fold-and-thrust belt, an increasing metamorphic gradient is also observed from the craton boundary (north), to the orogenic core (south) (Alkmim et al., 2017).

East of the Abre Campo shear zone and up to the current Atlantic coast, the core of the Araçuaí Orogen is mainly associated with amphibolite to granulite facies rocks (Alkmim et al., 2006; Tedeschi et al., 2016; Caxito et al., 2022). Post-metamorphic cooling occurred immediately after the metamorphic peak in the Ediacaran. The associated processes were primarily controlled by decompression during the orogenic collapse. U–Pb dating on monazite, titanite, and hydrothermal zircon indicates that post-metamorphic cooling and related hydrothermal fluid activity transpired along crustal-scale shear zones that crosscut the AWCO (Barrote et al., 2022). The orogenic core consists of two main structural segments (Fig. 2): (i) a northern segment following the trace of the Rio Pardo salient and the Itapebi shear zone, dominated by both west- and east-verging shear zones (Alkmim et al., 2006); and (ii) a southern segment containing a system of large-scale NNE-trending dextral strike-slip shear zones (Trompette et al., 1993). Of the latter, the Manhuaçu, Guaçuí, and Batatal shear zones are prominent examples (Fig. 2; Cunningham et al., 1998; Alkmim et al., 2006). From Vitória city on the Atlantic coast, the NNW-trending Vitoria-Colatina fracture zone represents a later-stage set of faults that cut across the earlier structural fabric described above (Fig. 2; Fleck et al., 2014).

2.3. The Araçuaí Orogen as the basement of the Mesozoic – Cenozoic Atlantic passive margin

On the Brazilian Atlantic margin, the Espirito Santo, Mucuri, and Cumuruxatiba basins were formed by continental rifting in the AWCO and related fragmentation of West Gondwana. In general, four phases characterize the tectonic and sedimentary development of these basins: Pre-Rift, Rift, Transitional, and Drift (Fig. 3; e.g., Vieira et al., 1994; Cainelli and Mohriak, 1999; Mohriak et al., 2002, 2008).

The Pre-Rift phase (Late Jurassic to Early Cretaceous) marks the onset of lithospheric extension and the thinning of the continental crust and upper mantle in this portion of Western Gondwana. The Afro-Brazilian depression was formed due to this extension and subsidence, which allowed continental sedimentation to accumulate (Cainelli and Mohriak, 1999). The Pre-Rift depositional record is recognized in the Monte Pascoal and Porto Seguro formations in the Cumuruxatiba Basin (Fig. 3; Rodovalho et al., 2007).

The Rift phase is marked by the development of the volcanic-sedimentary record during the Early Cretaceous. Throughout this period, crustal stretching caused mechanical subsidence, resulting in the formation of horsts and grabens. Deep tectonic basins were developed in which lakes were accommodated and filled with Neocomian to Barremian siliciclastic (Cricaré Formation) and volcanic (Cabiúnas Formation) deposits (Fig. 3; Mohriak et al., 2002).

A large sag-type basin formed during the Aptian, marking the beginning of the Transitional phase. This period is characterized by the shift from continental sedimentation of the Mucuri Formation to the marine evaporitic deposits of the Itaúnas Formation (Fig. 3; Henry and Brumbaugh, 1995; Henry et al., 1996; Mohriak et al., 2008).

The Drift phase is the last and current phase of the tectonic evolution of the Espírito Santo, Mucuri, and Cumuruxatiba basins. It is characterized by thermal subsidence in association with halokinesis and magmatic events, in which marine sedimentation predominated (e.g., França et al., 2007a,b). During the first stages of the Drift phase, active spreading centers evolved along the mid-Atlantic Ridge (Chang et al., 1992), where sandstones (São Mateus Formation) and Albian carbonates (Regência Formation) were deposited in a shallow marine platform environment (Fig. 3). In the Late Cretaceous, sedimentation of the Urucutuca Formation, characterized by claystones and turbiditic sandstones, revealed an increase in ocean depth. From 60 Ma to 40 Ma, several magmatic events associated with the Abrolhos volcanic complex affected the Espírito Santo, Cumuruxatiba, and, especially, the Mucuri basins (de Almeida, 1961; de Almeida et al., 1996; Sobreira and Szatmari, 2003; Sobreira and França, 2006; Stanton et al., 2022). The Abrolhos magmatism led to the development of the continental shelf and salt tectonics, forming several folds and faults in these basins (França and Ragagnin, 1996; Mohriak et al., 2008; Ferreira, 2010; Ferreira et al., 2014; Strozyk et al., 2017; Zhang et al., 2022).

In the Eocene, following the Abrolhos magmatic activity, a broad regressive phase began in these basins, which lasts until the present day, as indicated by the shallow water carbonate deposits of the Caravels Formation, and siliciclastics deposits from the Barreiras Group and Rio Doce Formation (França et al., 2007a, b). In the tablelands near the upper course of the Jequitinhonha River (Fig. 2), deep inland, terrigenous deposits of the São Domingos Formation are considered synchronous equivalents of the coastal deposits of the Barreiras Group. They outcrop on laterized plateaus, considered to be remnants of planation surfaces (Saadi, 1995; Pedrosa-Soares, 1997).

2.4. Available low temperature thermochronology data

Over the last two decades, seven low-temperature thermochronology studies analyzing samples from the Araçuaí Orogen were published. The AFT method was used in the vast majority of these studies, and >140 individual AFT ages were reported in total (Fig. 2 and Supplementary Data). In addition, two studies applied the apatite U-Th-Sm/He (AHe) technique on samples collected in the Araçuaí Orogen rocks (Van Ranst et al., 2020a; Amaral Santos et al., 2022). However, the AHe results reported suffered from overdispersal of individual ages or proved inconclusive (see Van Ranst et al., 2020a, for an overview). For that reason, these AHe data will not be discussed further in this contribution.

A significant portion of the studies mentioned above explored a profile across the Araçuaí Orogen from the east coast near Vitória to Serra do Caparaó and the Quadrilátero Ferrífero up to the boundary with the SFC (Fig. 2; Carmo, 2005; Van Ranst et al., 2020a; Fonseca et al., 2021; Fonte-Boa et al., 2022). A clear increase in the numerical values of the AFT ages is observed from the coast (Paleogene AFT ages) up to the craton (up to Early Jurassic AFT ages). For instance, Fonseca et al. (2021, 2022) and Amaral-Santos (2019) report similar Early Cretaceous AFT ages (~125–200 Ma) in the proximity of the craton along the Espinhaço Range. These AFT ages contrast with the Late Cretaceous and Paleocene (~60–125 Ma) ages obtained in the southeastern area (Jelinek et al., 2014; Van Ranst et al., 2020a). In this context, Fonseca et al. (2021) hypothesized that the exhumation of the Araçuaí Orogen has been primarily controlled by the presence of the stiff cratonic lithosphere at the edges of the orogen, which acts to mitigate surface uplift and subsequent denudation.

Overall, the low-temperature thermochronological studies in the Araçuaí Orogen identify two main events of basement cooling: (i) from the Early Cretaceous to the Cenomanian, related to the break-up of West Gondwana and inception of the south Atlantic Ocean; and (ii) from the Late Cretaceous to the Paleocene, associated with post-rift tectonic reactivation of the margin, resulting from either isostatic rebound (e.g. Jelinek et al., 2014) or far-field stresses transmitted from the Andes (e.g. Van Ranst et al., 2020a). The occurrence and significance of a third cooling event in the Neogene is still a matter of debate since this signal is constrained from thermal history modelling in temperatures below the sensitivity limit of the method (e.g., Jelinek et al., 2014; Van Ranst et al., 2020a; Fonseca et al., 2021).

3. Material and methods

3.1. Sampling

Our sampling strategy was designed to regionally extend previous low temperature thermochronology datasets in order to cover the Araçuaí Orogen's entire expanse. Provided that the vast majority of the available data was obtained from the southern Araçuaí Orogen and the Paramirim aulacogen region (Fonseca et al., 2022), we therefore focused sample collection in the northern and central areas of the Araçuaí Orogen (Fig. 2). Furthermore, we preferentially sampled lithologies that are known to provide satisfactory apatite yields and quality. On the northern part of the area, facing the Mucuri and Cumuruxatiba basins (Fig. 2), appropriate sample sites proved to be limited, due to the large area covered by the Barreiras Group sediments (~50–150 km of coast). A total of 29 samples from Neoproterozoic and Cambrian igneous and metamorphic rocks were eventually processed for AFT analysis. Their location in the area is shown in Fig. 2, and their coordinates can be consulted in Table 1.

3.2. AFT analysis

The apatite fission-track (AFT) method is based on the natural fission decay of ^{238}U. This spontaneous fission produces damage trails (fission tracks) in the apatite lattice where U is present as a trace element. As fission tracks accumulate over time at a constant rate, the number of tracks per unit area is a measure for the AFT age. The AFT age represents a cooling age as fission tracks in apatite only become stable and accumulate at temperatures lower than ~ 120 °C. This corresponds to about 4 km of crustal depth when considering a continental crustal geothermal gradient of 25–30 °C/km. Between ~ 120 °C and 60 °C, fission tracks in apatite are retained but are shortened due to thermally driven restoration of the crystal lattice. This temperature interval is called the apatite partial annealing zone (APAZ; Wagner and van den Haute, 1992 and references therein). At temperatures higher than ~ 120 °C, fission tracks in apatite are completely annealed over geological time scales (e.g., Gleadow and Brown, 2000). Consequently, AFT length is a measure of the paleo-temperatures that the apatite-bearing rock experienced through its evolution in the crust (Gleadow et al., 1986; Ketcham et al., 2007). The annealing behavior and shortening of apatite fission tracks can thus be used for thermal history modelling (e.g. Laslett et al., 1987; Ketcham, 2005; Gallagher, 2012).

For this study, apatite grains were concentrated from the rocks by conventional crushing and magnetic and heavy liquid separation. Apatite grains were then hand-picked and mounted in Struers CaldoFix-2 epoxy resin, after which they were grinded on SiC paper and polished using diamond suspension (6 μm, 3 μm and 1 μm). Mounts were etched in a 5.5 M HNO_3 solution for 20 s at 21 °C (Donelick, 1991), in order to reveal the spontaneous (fossil) tracks for optical microscopy. U-free mica was attached on top of each mount as an external detector (ED) (Fleischer et al., 1975; Hurford and Green, 1982). Thermal neutron irradiations were performed at the BR1 nuclear reactor (Belgian Nuclear Research Centre SCK, Mol; De Grave et al., 2010). IRMM-540 dosimeter glass was used for monitoring the thermal neutron fluence (De Corte et al., 1998). After irradiation, induced fission tracks in the mica ED were revealed by etching with 40% HF for 40 min at 20 °C. The amount of induced tracks is a measure for the current U-concentration in the apatites.

For each sample, spontaneous and induced track densities of 20 apatite grains were obtained using a motorized Nikon Eclipse Ni-E microscope with a DS-Ri2 camera attached at a 1000 × magnification and using the Nikon-TrackFlow protocol (Van Ranst et al., 2020b). Central age calculation and Chi-squared (χ^2) homogeneity test parameters (Galbraith, 2005) were calculated using the IsoplotR software (Vermeesch, 2018) with an overall weighted mean zeta value of 327.8 ± 3.4 a·cm^2 (analyst AF) based on multiple apatite (Durango and Fish Canyon Tuff) age standards (Hurford and Green, 1983). Lengths of confined apatite fission tracks (Gleadow et al., 1986) and the angle between the tracks and the crystallographic *c*-axis were measured using the same microscopic setup. We aimed at measuring 100 track lengths in each sample to construct a representative AFT length-frequency distribution, although such a target was not attainable in some

Table 1
Sample localities (in World Geodetic System – WGS84), *Z*: elevation above sea level, and lithology. AFT age and length data: *n* is the number of counted grains; ρ_s, ρ_i, and ρ_d represent the density of spontaneous, induced tracks and induced tracks in an external detector (ED) irradiated against dosimeter glass respectively (all expressed as 10^5 tracks/cm^2). The ρ_d values are interpolated from data from regularly spaced glass dosimeters in a single irradiation container. N_s, N_i, and N_d are the number of counted spontaneous, induced tracks and induced tracks in the ED irradiated against the dosimeter glass. N_d is an interpolated value (as for ρ_d). P(χ^2) is the chi-squared probability that the dated grains have a constant ρ_s/ρ_i-ratio. A ζ-value (OWMZ) of 327.8 ± 3.4 a·cm^2 (analyst AF) was used for the calculation of the AFT central age (in Ma) based on Durango and Fish Canyon Tuff age standards and the IRMM-540 dosimeter glass. AFT length data are reported as raw mean track length (MTL in μm) and *c*-axis projected mean track length (MTL_p in μm, Ketcham et al., 2007) with standard deviation σ, and σ_p (in μm), obtained from the measurement of a number (n_c) of natural, horizontal confined tracks. Angles between the *c*-axis and measured confined tracks were acquired in order to apply the *c*-axis correction. D_{par} (in μm) was determined as the mean of 100 measurements of the track etch pit diameter parallel to the crystallographic *c*-axis. x means "no data".

Sample	Latitude (°)	Longitude (°)	Z (m)	Lithology	n	ρ_s	N_s	ρ_i	N_i	ρ_d	N_d	P (χ^2)	AFT central age (Ma)	1 s.e. (AFT age)	n_c	MTL (μm)	σ (MTL) (μm)	MTL_p (μm)	σ_p (MTL) (μm)	D_{par} (μm)
TJ 37	−15.8828	−41.4217	769	granite	20	31.498	3221	19.458	1986	4.863	2415	0.36	128	5	100	12.2	1.7	13.6	1.3	1.96
TJ 39	−16.0485	−41.7754	720	granite	20	7.509	825	5.364	576	4.850	2408	0.44	113	7	100	12.7	1.8	14.1	1.2	1.56
TJ 41	−16.2505	−41.4712	606	granite	20	8.959	1024	7.148	845	4.836	2402	0.34	95	5	x	x	x	x	x	1.50
TJ 42	−16.3589	−41.4707	555	granite	20	6.776	823	5.387	667	4.823	2395	0.76	97	6	100	13.0	1.7	14.2	1.2	1.28
TJ 43	−16.4389	−41.4985	347	granite	20	4.970	480	5.230	488	4.809	2389	0.36	78	6	52	12.2	1.5	13.7	1.1	1.27
TJ 44	−16.5755	−41.5045	262	granite	20	8.529	794	8.101	953	4.796	2382	0.23	82	5	x	x	x	x	x	1.98
TJ 45	−16.6662	−41.5023	325	granite	20	8.349	955	6.180	700	4.922	2475	0.55	109	6	100	12.6	2.0	14.1	1.3	1.70
TJ 46	−16.8172	−41.4706	500	granite	20	2.365	393	2.061	346	4.911	2470	0.98	91	7	100	12.9	1.7	14.3	1.2	1.52
TJ 47	−16.9107	−41.4706	555	granite	20	16.610	2026	9.849	1177	4.900	2464	0.12	137	7	100	12.3	1.9	13.9	1.3	1.30
TJ 48	−17.0002	−41.4469	614	granite	20	8.276	831	5.488	562	4.182	2102	0.46	101	7	x	x	x	x	x	1.26
TJ 50	−17.2452	−41.5017	693	granite	20	18.334	2134	11.073	1298	4.188	2104	0.20	112	5	100	12.6	1.8	14.0	1.2	1.50
TJ 53	−17.4293	−41.8089	830	granite	20	19.872	2259	94.850	1091	4.191	2105	0.12	141	7	100	11.4	1.7	13.3	1.2	1.53
TJ 54	−17.5111	−41.8899	830	granite	20	13.376	1441	8.702	934	4.195	2106	0.62	105	5	100	11.4	2.0	13.2	1.4	1.84
TJ 55	−17.8936	−42.3801	660	gneiss	20	7.525	802	4.634	491	4.198	2107	0.66	111	7	100	12.4	1.8	14.0	1.1	1.86
TJ 56	−17.9806	−42.3902	475	gneiss	20	11.072	1597	7.773	1106	4.201	2109	0.38	99	5	100	12.0	1.8	13.6	1.2	1.78
TJ 57	−18.1048	−42.4122	567	gneiss	20	5.763	961	4.087	704	4.205	2110	0.14	96	6	100	12.4	1.8	13.9	1.1	1.47
TA 05	−16.7253	−41.8992	281	schist	20	8.662	1121	4.930	637	4.208	2111	0.19	120	7	x	x	x	x	x	1.33
TA 07	−16.6107	−41.7562	299	granite	20	25.582	2161	16.270	1415	4.211	2113	0.22	105	5	100	12.0	1.8	13.7	1.2	1.37
TA 08	−16.5795	−41.6126	284	granite	20	22.758	1575	12.882	886	4.214	2114	0.68	122	6	100	12.5	1.9	14.0	1.3	1.36
TA 13	−16.4232	−40.9552	220	granite	20	29.495	2053	23.436	1628	4.218	2115	0.22	87	4	85	11.6	1.8	13.4	1.1	1.29
AL 03	−16.4262	−41.0116	212	migmatite	20	31.420	2288	15.161	1109	4.221	2117	0.93	141	6	100	12.5	1.8	13.9	1.3	1.35
AL 04	−16.5842	−41.7380	270	granite	20	30.147	2490	15.960	1327	4.233	2122	0.70	129	5	100	12.3	1.7	13.8	1.2	1.44
AL 05	−16.8616	−41.9465	570	granite	20	27.075	2370	16.151	1449	4.237	2123	0.32	113	5	100	12.1	1.5	13.8	0.9	1.47
AL 06	−16.8751	−41.9409	780	volcanoclastic	20	27.246	2136	14.696	1156	4.240	2124	0.32	127	6	100	12.1	1.6	13.7	1.1	1.30
AL 07	−17.9771	−43.1204	754	granite	20	11.206	1233	4.893	536	4.243	2125	0.07	167	13	50	12.2	2.0	13.7	1.3	1.37
AL 08	−18.6652	−43.0731	730	gnaisse	20	9.928	1489	6.239	935	4.246	2127	0.71	110	5	100	12.8	1.7	14.2	1.1	1.24
AL 11	−16.0804	−42.2952	617	metaconglomerate	20	10.216	1062	4.422	480	4.249	2128	0.08	153	11	100	12.2	1.7	13.6	1.1	1.35
AL 12	−15.8382	−43.0630	650	granite	20	18.875	1342	8.715	647	4.252	2129	0.01	146	11	100	12.2	1.9	13.9	1.1	1.40
AL 13	−15.0631	−42.8019	703	gnaisse	20	21.168	1464	7.480	531	4.255	2130	0.20	191	12	85	11.6	1.6	13.4	1.1	1.29

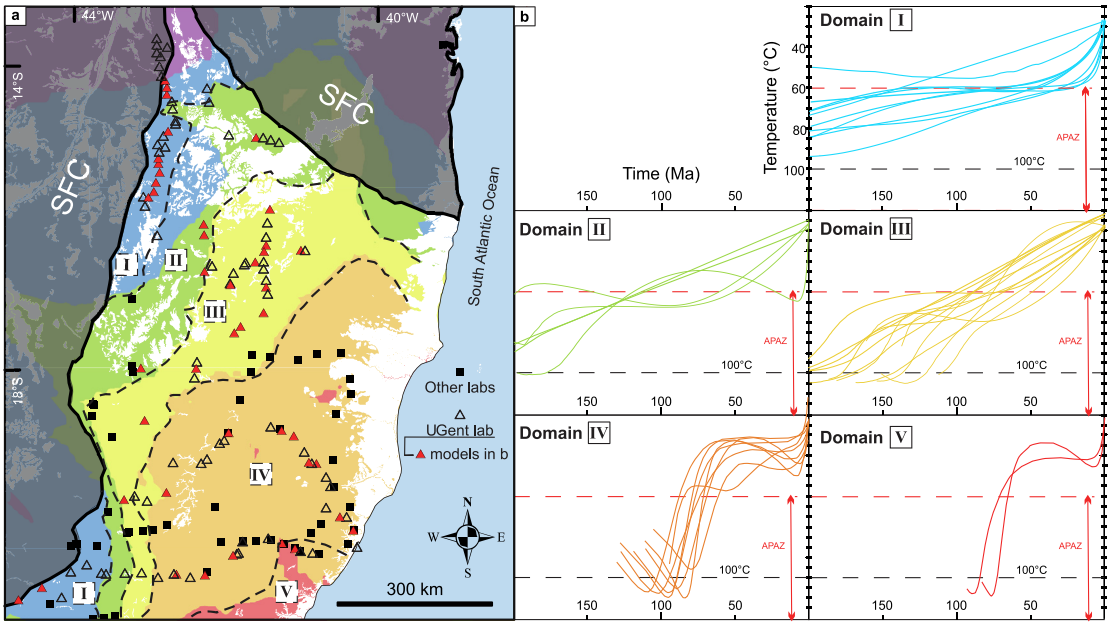

Fig. 5. (a) Map of exhumation domains in the Araçuaí Orogen based on the interpretation of AFT data. (b) Representative thermal history models for each domain computed using the QTQt software (Gallagher, 2012) and based on AFT results presented in this study. For further details on each model, see the Supplementary Data and the cited publications.

samples (Table 1). The etch pit diameter parallel to the crystallographic *c*-axis (D_{par}) (Donelick et al., 1999) was determined as the mean of 100 etch pit diameters per sample. D_{par} is a parameter use to describe the annealing kinetics of fission tracks in a particular apatite crystal (Donelick et al., 1999).

3.3. Kriging interpolation

In order to visualize patterns and clusters of AFT ages in the Araçuaí Orogen, we interpolated our AFT data in combination with the available AFT central age dataset of the Brazilian territory (Novo et al., 2021). We emphasize that a significant proportion of this AFT dataset available for the Araçuaí Orogen was acquired by the fission track laboratory at Ghent University in the past five years, using the same procedures and optical equipment as in this contribution (Fig. 5; Van Ranst et al., 2020a; Fonseca et al., 2021, 2022). Kriging was used for estimating a continuous surface of AFT ages from a limited set of AFT data. The kriging interpolation is a geostatistical method that assumes, in our case, that sampled rocks close in space have experienced similar thermal histories (Gallagher et al., 2005). That is, the kriging interpolation is based on the spatial arrangements of the data, such that, in general, the more distant mutual sample sites are, the smaller the chance is that they have to share the same time-Temperature (t–T) path. Kriging also takes into account clustering effects in data points such that clusters of points are weighted less heavily, aiming to minimize bias in the interpolation (Oliver and Webster, 2015). However, as with any interpolation method, kriging has a set of limitations (e.g., Oliver and Webster, 2015). For instance, kriging assumes uniformity in every direction, which is problematic when we have structural discontinuities such as faults or shear zones (Brown et al., 2001; Kohn, 2005). To minimize the chances of misinterpretation, we added the main tectonic structures in the map after interpolation (Fig. 4).

3.4. Thermal history modeling

For an eroding crust, quantifying the thermal history of a rock sample based on AFT data allows estimating the timing and magnitude of exhumation toward the surface (Braun et al., 2006). In this situation, the AFT data can, for example, be used as input data to generate inverse thermal histories using modeling software such as HeFTy (Ketcham, 2005) and QTQt (Gallagher, 2012). In this contribution, we used the QTQt software (Gallagher, 2012) to invert our AFT data and extract thermal histories for samples with >50 (mostly around 100) measured track lengths (Fig. 5). We employed a Markov Chain Monte Carlo search method for our inverse modeling, using 10^5 post-burn iterations. The t-T prior information for each sample was set to (central age ± central age) for time and 70 ± 70 °C for temperature. We used the D_{par} value as a kinetic parameter in the annealing model (Ketcham et al., 2007). Only the present-day temperature was set as an external constraint (i.e., 25 ± 15 °C). Modeling results for samples with sufficient track length data are presented in Supplementary Data.

4. Results

We present new AFT data from 29 samples, primarily from the northern Araçuaí Orogen. We summarize the AFT data in Table 1, while radial plots (Galbraith, 2005), track length histograms, thermal history models data and comparative graphs are available in the Supplementary Data. We also present the result of a comprehensive AFT data compilation from the entire Araçuaí Orogen through an interpolated kriging map (Fig. 4). We show thermal history model curves in Fig. 5 to characterize the exhumation of the orogen.

4.1. New AFT analysis

Most of the samples investigated in this study yield Cretaceous AFT central age ranging between 78 ± 6 Ma (AL 43) and 141 ± 7 Ma (TJ 53). Samples AL 07, 11, 12, and 13 produce older Jurassic AFT ages varying from 146 ± 11 Ma (AL 12) to 191 ± 12 Ma (AL 13). The location of these two latter sample sites are adjacent (<1 km) to sample sites discussed in Fonseca et al. (2022), and their result is indeed similar. Only sample AL 12 did not pass the χ^2 tests ($P(\chi^2) < 5\%$; Galbraith, 2005), while all the other samples show narrow single-grain age distributions. There is no apparent correla-

tion between AFT central age and elevation (Supplementary Data S.3). For four samples (TJ 41, TJ 44, TJ 48, and TA 05), we were unable to measure >50 confined track lengths. For the other 25 samples, the histograms generally present a unimodal distribution (Supplementary Data S.2) with mean track length (MTL) values falling within a relatively restricted range of 11.4 – 13.0 μm (not projected) and 13.2 – 14.2 μm (*c*-axis projected). The standard deviation of the MTL data is broad and varies between 1.5 and 2.0 μm, and decreases with *c*-axis projection, varying between 0.9 and 1.3 μm (Supplementary Data S.5). D_{par} values range from 1.24 to 1.98 μm, which indicates chlorine-poor apatite (Donelick, 1993). The D_{par} variation is not correlated with AFT central age (Supplementary Data S.6).

4.2. Spatial distribution of the AFT ages

Based on the AFT age distribution and sample locations, an interpolated AFT age map was produced (Fig. 4). The map is color-coded by age intervals corresponding to phases of rifting and separation between South America and Africa: (i) < 200 Ma, (ii) 200 – 150 Ma, (iii) 150 – 125 Ma, (iv) 125 – 100 Ma, (v) 100 – 75 Ma, and (vi) < 75 Ma. This interpolated map allows us to visualize the main trends of AFT age distribution in the Araçuaí Orogen with respect to the tectonic setting. The youngest ages are distributed close to the coast, mainly in the SE segment of the orogen. In turn, ages gradually increase towards the craton, progressively both in transversal (E to W) and parallel (S to N) directions from the coast.

Occasionally, samples with different ages occur as outliers owing to limitations of the kriging algorithm that does not consider sudden discontinuities in the data. In this situation, substantial differences in AFT ages in a very localized area can, for example, result from local tectonic structures. In any case, the interpolated map is consistent with the main AFT age trends and t-T models (section 4.3), demonstrating its usefulness in providing insights about exhumation patterns in the Araçuaí Orogen rocks and its tectonic and sedimentary significance.

From the interpolated map and considering the structural lineaments, we distinguish five "exhumation domains" in the Araçuaí Orogen (Domains I to V, Fig. 4). Domain I consists of regions along the SFC border with AFT ages older than 150 Ma. Domain II borders the SFC in the Espinhaço Range region and is defined by ages between 150 and 125 Ma. Domain III comprises sample sites with AFT ages from 125 to 100 Ma and is primarily located in the northern part of the Araçuaí Orogen, hence including most of our new data. AFT ages from 100 to 75 Ma dominate Domain IV, which occupies most of the coastal region and the Doce River valley. Finally, Domain V comprises the SE coastline of the orogen, facing the Campos Basin, and shows AFT ages < 75 Ma. In general, the boundaries of the domains are more precisely outlined in the southern part of the Araçuaí orogen compared to the north because of the lower density of AFT samples in the latter.

4.3. Thermal history modeling and exhumation domains

Using the QTQt software (Gallagher, 2012), 'expected' time-Temperature (t-T) paths for our samples were grouped per exhumation domain in Fig. 5. These thermal history models reveal a substantial increase in cooling rate from Domain I to Domain V. Models from Domain I display relatively slow cooling through the APAZ from > 200 Ma to 60 Ma, with an average cooling rate of 0.20 °C/Ma. In some models, such prolonged residence time in the APAZ is followed by an abrupt increase in the cooling rate (~0.67 °C/Ma) during the Neogene. Domains II and III present moderate cooling rates through the APAZ, with Domain II featuring more complex thermal histories, while Domain III models, in general, show steady cooling since the Early Cretaceous (~0.40 °C/Ma). For Domain IV, most samples record a heating phase at ~ 130 – 90 Ma from ~ 90 to 110 °C, with subsequent rapid cooling (~18 °C/Ma) reaching the upper APAZ at ~ 105–75 Ma. The two models for Domain V record a similar rapid cooling (~18 °C/Ma) through the APAZ, reaching the upper APAZ later, i.e., between ~ 95 and ~ 75 Ma. The thermal history models are internally consistent for each exhumation domain but significantly differ between different domains.

5. Discussion

We discuss the cooling of the Araçuaí Orogen rocks and its exhumation based on the new dataset presented in this work, along with published AFT data from other parts of the orogen. The thermal history models reveal that the majority of samples cooled through the APAZ (~60 – 120 °C) between the Mesozoic and Cenozoic at variable cooling rates (Fig. 5). All the samples analyzed in this contribution consist of (Pre)Cambrian crystalline basement rocks of the orogen that were thus formed long before this Mesozoic – Cenozoic final cooling within the passive margin context.

We interpret the Mesozoic – Cenozoic cooling events of the basement rocks as a result of their exhumation due to regional denudation. There is no geological evidence suggesting that the upper crust of the Araçuaí Orogen was substantially heated during the Mesozoic – Cenozoic, and hence explaining the cooling of the Araçuaí basement as a response to a prior thermal event, is not substantiated. Elevated heat flow during the rifting and accompanying asthenospheric upwelling or subsurface magmatic activity has limited or no repercussions on the upper continental crust away from the rift axis (Morgan, 1983; Gallagher et al., 1994; Cogné et al., 2011). For instance, the anomalously high heat flow and geothermal gradient in the East African rift are limited to a distance tens of kilometers from the main fault zone (Lucazeau, 2019; Macgregor, 2020). Measurements of the heat flow of the Red Sea also corroborate that the thermal influence of the rifting decreases rapidly with the distance from the rift axes (Lucazeau, 2019). The areas of the Araçuaí Orogen that were located at a close distance from the rift axis now form part of the covered, offshore passive margin. The onshore area investigated here was positioned more distant from the axis. Furthermore, the emplacement of Cretaceous mafic dikes onshore (~130 Ma, Ar-Ar; Coelho and Chaves, 2017) and the Abrolhos magmatism (~69 – 32 Ma; Ar-Ar and K-Ar; Stanton et al., 2022) likely had minor potential to heat host rocks at a distance from the intrusion itself. This is indicated by previous low-temperature thermochronological investigations in basement rocks nearby Large Igneous Provinces (e.g., Paraná-Etendeka; Deccan LIP's), suggesting only a minor direct influence of plume-induced heating (e.g., Sahu et al., 2013; Amaral-Santos et al., 2019; Fonseca et al., 2020).

5.1. Timing and causes of major Mesozoic – Cenozoic exhumation events in the Araçuaí Orogen

The timing of major Mesozoic – Cenozoic exhumation in the eastern South America based on thermochronometric data has been discussed in several papers (Jelinek et al., 2014; Amaral-Santos et al., 2019; Van Ranst et al., 2020a; Fonseca et al., 2021, 2022; Fonte-Boa et al., 2022). Based on the new AFT data and thermal history modeling, we identify three major periods of denudation in the Araçuaí Orogen with consequent exhumation and hence rock cooling: (i) Jurassic – Hauterivian (200 – 130 Ma); (ii) Barremian – Albian (130 – 100 Ma), and (iii) Late Cretaceous – Paleocene (100 – 60 Ma). The first two events were combined in

earlier publications as the Early Cretaceous to Cenomanian event (see section 2.4). However, because the environmental and erosion conditions varied significantly during that time, from an intracontinental rift to passive margin systems, we differentiate between them, subdividing the discussion into the Jurassic – Hauterivian and the Barremian – Albian time-frames. Furthermore, the data does not show cooling in the APAZ during the Late Eocene or Neogene, suggesting that the magnitude of Late Cenozoic erosion was negligible in our study area in the northern Araçuaí Orogen and must have been limited to <1 km (considering a geothermal gradient of 25 °C/km).

5.1.1. Jurassic – Hauterivian (200 – 130 Ma, Pre-Rift)

Samples from Domains I, II, and III show an initial exhumation during the Jurassic – Hauterivian (Figs. 4 and 5), which includes all of the new samples analyzed in this study. The age range of initial cooling to within the APAZ varies between ~ 200 Ma and 130 Ma, with increasing cooling rates from Domain I to Domain III. In these domains, the obtained results dominantly yield pre-Atlantic AFT ages (>115 Ma; Heine et al., 2013). The majority of these samples remained within the APAZ for a relatively long time before their final exhumation (and hence cooling), resulting in significant partial annealing and shortening of the fission tracks, which led to shorter MTL values (Amaral-Santos et al., 2019; Fonseca et al., 2021, 2022) and age variability (e.g., Malusà and Fitzgerald, 2019). In general, the cooling rate is slow (0.1 °C/Ma) to moderate (0.4 °C/Ma) and steady throughout the Jurassic (Fig. 5). Domains IV and V probably also experienced this cooling phase, yet it is no longer preserved as more recent exhumation has removed the overlying basement with this signal, exposing deeper sections of the crust.

In the interior of West Gondwana, the Jurassic – Hauterivian period is characterized by the Pre-Rift phase with the inception of extensional stresses and development of the Afro-Brazilian depression in the central and northern parts of this paleocontinent (Cesero and Ponte, 1972; Ghignone, 1979; Kuchle et al., 2011). At that time, flexural subsidence in this continental basin and consequent relative uplift in the adjacent areas would have increased exhumation and erosion in most of the Araçuaí Orogen, due to increased hillslope and river erosion power. In our thermal history models (Domains I, II, and III), we observe that this event is characterized by a slow and protracted exhumation rates. In intracratonic basins, such as the Afro-Brazilian, normal faults and strong displacements were uncommon (Sloss and Speed, 1974; Sloss, 1988; Allen and Armitage, 2012), resulting in a shallow basin (Silva et al., 2012) which resulted in relatively slow denudation of the source areas.

Remnants of Jurassic – Hauterivian deposits from the Afro-Brazilian basin are scarce due to their restricted spread and limited sedimentary thickness. Nonetheless, they are found underneath Early Cretaceous rift sediments in several basins of the northeastern Brazilian passive margin (e.g., Cumuruxatiba, Almada, Camamu, Sergipe-Alagoas basins) and in the onshore Recôncavo-Tucano-Jatobá basin (Fig. 1; Ghignone, 1979; Santos et al., 1990; Magnavita, 1992; Figueiredo et al., 1994). These deposits are exclusively continental, with fluvial, aeolian, and lacustrine systems genetically related to an incipient crustal extension (Ghignone, 1979; Kuchle et al., 2011). In Jurassic fluvial strata, paleocurrent data (n > 350, Kuchle et al., 2011) suggest source areas to the south-southwest of the present-day basin, which coincides with the position of the Araçuaí-West Congo orogen (AWCO) at that time (Scherer et al., 2007). Furthermore, U–Pb and Lu–Hf isotopic analysis on detrital zircons from Jurassic fluvial deposits of the Camamu Basin provide strong evidence of the contribution of the AWCO region as a source area (Bertotti et al., 2014). The detrital zircon U–Pb age spectra show clear Neoproterozoic age peaks (with main peaks at 500 Ma to 600 Ma). These correspond to the timing of AWCO pre-, syn- and post-orogenic magmatism (e.g., Pedrosa-Soares et al., 2008, 2011, 2020). Therefore, the provenance and thermochronological data suggest that bedrock river incision in the Araçuaí Orogen actively contributed to the exhumation of the orogen on the one hand and to the influx of sediments into the northern basins on the other (Caixeta et al., 2007).

The Paraná Basin, located southwest of the orogen, represents another potential depocenter that could have received sediments from nearby paleo-highs such as the Araçuaí Orogen. In the Paraná Basin, the Late Jurassic deposits (e.g., Botucatu Formation) contain both aeolian and thin fluvial sequences (Scherer, 2000; Scherer and Lavina, 2006; Moraes and Seer, 2018). The fluvial sequences were mostly locally sourced, reworked from underlying Paraná Basin units (Bertolini et al., 2021). In contrast, the aeolian sediments received contributions of the Neoproterozoic – Cambrian granitoids from the north, as suggested by paleowind patterns and detrital zircon U–Pb isotopic data (520 – 750 Ma dominant population) (Scherer and Goldberg, 2007; Bertolini et al., 2021). Although the Araçuaí Orogen might have been a source area for these, and cannot be excluded, it is more reasonable that the Ribeira Orogen was the primary source region given its closer proximity (Bertolini et al., 2021).

5.1.2. Barremian – Albian (130 – 100 Ma, Rift to Transitional)

Inverse thermal history models for samples from Domains I, II, and III show a Barremian to Albian slow to moderate cooling within the APAZ. Jelinek et al. (2014) and Carmo (2005) also reported this cooling phase in their study (Fig. 2). Similar to observations for the Jurassic – Hauterivian cooling, thermal history models for samples in Domains IV and V have not preserved this Barremian – Albian signal because posterior erosion has exposed deeper parts of the crust.

This cooling phase is coeval to the onset of mechanical subsidence in the basin, with the nucleation and displacement of a complex system of normal faults. In the Barremian, i.e., Rift phase, the most intense phase of rifting and associated fault activity eventually broke up the AWCO into its two counterparts (Mohriak et al., 2002; Heine et al., 2013). High rates of crustal stretching and the development of intra-continental rifts culminated in the magmatism of the Cabiúnas Formation (Espírito Santo basin) at ~ 130 Ma. Previous research relates the Early Cretaceous cooling event in the Araçuaí Orogen with a denudational event triggered by the surface uplift of the rift flanks and shoulders (Carmo, 2005; Jelinek et al., 2014; Fonseca et al., 2021). Numerical modeling by Rouby et al. (2013) demonstrates that uplifted rift flanks can generate, on average, a total denudation of about 1.6 km in the hinterland, reaching up to 2.6 km at the location of maximum rift shoulder uplift. Furthermore, the incipient northward opening of the South Atlantic Ocean reached our study area at around 115 Ma ago (Heine et al., 2013), establishing a new base level for continental erosion represented by the newly formed basins such as the Espírito Santo, Mucuri, and Cumuruxatiba basins. In this situation, the prominent role of erosion and the reorganization of the preexisting drainage networks due to the newly formed base level is supported by the offshore *syn*-rift and transitional deposits (Cricaré and Mucuri Fms.). These deposits comprise up to 5500 m of alluvial and fluvial-lacustrine sediments (Vieira et al., 1994; Mohriak, 2003; França et al., 2007a,b). Hence, our data agrees with previous interpretations that both the Barremian extensional tectonism and the Albian shift from continental to a marine base level have resulted in increased rates of bedrock channel incision and cooling of the Araçuaí Orogen rocks through its erosional exhumation (Jelinek et al., 2014; Fonseca et al., 2021; Fonte-Boa et al., 2022).

5.1.3. Late Cretaceous – Paleocene (100 – 60 Ma, Drift)

Thermal history models from Domains IV and V show a rapid cooling phase during the Late Cretaceous and Paleocene. Overall, samples from these domains yield AFT ages ranging from ~ 90 Ma to 65 Ma with high MTL values (>13.5 μm) and a narrow standard deviation, implying a rather rapid basement cooling (Green et al., 1989). According to the numerical modeling from Rouby et al. (2013), within 10 to 20 Ma after initiation, the rift topography is erased due to erosion, and the rift shoulders erosion is thus unable to account for the rapid basement cooling events that occurred much later after the break-up as observed here. The Late Cretaceous – Paleocene cooling phase is younger than the rifting event, which suggests that the margin experienced substantial late post-rift denudation (e.g., Gallagher et al., 1994; Cogné et al., 2011; Jelinek et al., 2014; Van Ranst et al., 2020a).

The passive margin of South America experienced several magmatic events and processes of intra-continental basin subsidence in the Late Cretaceous and Early Cenozoic (Batezelli and Ladeira, 2016). For example, in the Ribeira Orogen, several studies document a phase of intense erosion related to an episode (or episodes) of post-rift reactivation. During this phase, the Serra do Mar Range and the Cenozoic Rift System of Southeastern Brazil were formed (Fig. 1; e.g., Franco-Magalhaes et al., 2010, 2014; Hiruma et al., 2010; Cogné et al., 2011, 2012; de Oliveira et al., 2016; Souza et al., 2021). Several authors also hypothesise that in the Araçuaí Orogen post-rift cooling events can be explained by differential vertical motion between basement blocks (e.g., Jelinek et al., 2014; Van Ranst et al., 2020a; Fonseca et al., 2021; Fonte-Boa et al., 2022). In this scenario, the contemporaneous turbiditic sandstones recorded in the offshore Espírito Santo basin corroborate increased sedimentary input and erosion during that time (e.g., Gamboa et al., 2010; Nascimento et al., 2020). There are also numerous alkaline igneous intrusions both onshore and offshore in this segment of the Brazilian margin. These intrusions are dated between 88 and 76 Ma (Thomaz Filho et al., 2005; Geraldes et al., 2013), indicating potential tectonic activity of the margin.

The flexural-isostatic rebound of the lithosphere due to continental denudational unloading and offshore sediment loading is routinely invoked as an explanation for post-rift tectonism in the coastal segments of the Brazilian passive margin (Gilchrist and Summerfield, 1990; Summerfield, 1991; Gilchrist et al., 1994; Bishop, 2007; Jelinek et al., 2014). Some modeling studies suggested that passive margins experiencing such flexural response are expected to have accumulation and accommodation rates decreasing exponentially through time (e.g., Rouby et al., 2013), which is not the case for the tectonic and sedimentary evolution of the Eastern Brazilian passive margin (Mohriak et al., 2008). Thus, other mechanisms must also be taken into account to explain the Late Cretaceous to the Paleocene cooling. Likely candidates include climate change scenarios or significant discrete river reorganization events, both capable of explaining an increase in sediment influx and loading in the coastal basins that, in turn, could result in a critical flexural-isostasy uplift response of the margin. Although our study area lacks well-defined paleoclimate data from the Late Cretaceous to the Paleocene, there is no evidence of a more humid or wetter climate during this particular period. On the contrary, deposits in interior basins, such as the Bauru Basin for example, indicate deposition under semi-arid conditions (Garcia et al., 2005; Fernandes and Ribeiro, 2015; Menegazzo et al., 2016), suggesting a dryer climate at this time. Furthermore, on the Eastern Brazilian margin, isostatic flexural responses are likely to be a much more protracted and self-sustained process than a discrete, forceful and intermittent mechanism (Fonte-Boa et al., 2022). Hence, the subsidence and sedimentary accumulation history observed during the post-rift phase likely suggests that the margin must have undergone additional tectonic events.

We attempt to evaluate the Late Cretaceous to the Paleocene phase in a broader tectonic context. Late Cretaceous deposits in the Bauru, Sanfranciscana, Parecis, and Solimões basins (Fig. 4) are contemporaneous with the early stages of the Andean uplift (Mochica and Peruvian phases), indicating a possible influence of intraplate compressive stresses transmitted from the Andean orogeny to the intracontinental interior (Menegazzo et al., 2016). Other evidence of continental stress transmission on larger scales from plate boundaries during the Late Cretaceous – Paleocene is the occurrence of synchronous erosion events in different parts of the continent, such as on the northeast coast of Brazil (Morais Neto et al., 2009). Therefore, compressive stress propagation from the Andean margin and the ridge-push of the Atlantic Ocean spreading zone seem a reasonable driving forces for the Late Cretaceous – Paleocene tectonic reactivations of the Eastern Brazilian passive margin (e.g., Cogné et al., 2011, 2012; Van Ranst et al., 2020a; Fonseca et al., 2021). Although there is compelling evidence of far-field stress transmission (Craddock et al., 2017; Silva et al., 2018; Cunningham et al., 2021), our understanding of how the stresses reach these distal areas far from the plate boundary and how they influence the continental crust is still limited (e.g., Silva et al., 2018).

Other second-order and more localized factors might also influence post-rift tectonic reactivation with rock uplift. Among these processes, we highlight the potential influence of convection cells in the mantle (e.g., Sacek, 2017), magmatic underplating (e.g., Gallagher et al., 1994; Hackspacher et al., 2004), and mantle plume activity (e.g., Franco-Magalhaes et al., 2010, 2014). All these processes are expected to promote a long-wavelength up-warp of the margin, yet they cannot explain an exhumation event of this magnitude, i.e., 60 °C of cooling, constrained by our models (Rouby et al., 2013; Fonte-Boa et al., 2022).

5.2. Spatial patterns of Mesozoic – Cenozoic exhumation and control of tectonic inheritance

The kriging interpolation of the AFT age and the thermal history modeling data from the Araçuaí Orogen allows to visualize the spatial pattern of denudation/exhumation during the Mesozoic – Cenozoic, in a passive margin setting (Fig. 5). The configuration of the exhumation domains delineated in the interpolated map demonstrates that the exhumation pattern in the Araçuaí Orogen does not simply reflect the development of a marginal scarp gradually retreating towards the continental interior. Our data suggest that the distance from the craton, rather than the distance to the coast, exerts the primary influence in the arrangement of the exhumation domains (comparative plots in the Supplementary Data). For instance, the basement cooling rates gradually increase with distance from the SFC. In turn, the slowest rates of cooling (Domain I) are localized in the border zone with the craton (Jelinek et al., 2014). More rapid cooling rates are found in the southeastern area, away from the stiff lithosphere (Van Ranst et al., 2020a). These findings agree with the hypothesis put forth by Fonseca et al. (2021) that the fundamental factor influencing the exhumation of the eastern Brazilian coast is lithospheric stiffness and rigidity. The proximity to the SFC's rigid lithosphere likely mitigates surface uplift and, as a result, the erosion and exhumation of the basement since the onset of rift tectonics. Van Ranst et al. (2022) reached a similar conclusion for the West Congo Belt, i.e. the African counterpart of the Araçuaí Orogen.

In general, the domains' limits seem to follow the main structure of the orogen, i.e., with an N – S orientation in the south and curving to the NE in the north until it reaches an E – W orientation and then ultimately a SE direction on the northeastern coast (Fig. 4; Alkmim et al., 2017). In view of this, the orogen's intracontinental zone in the north (e.g. Cruz et al., 2015; Fig. 2; Domains I,

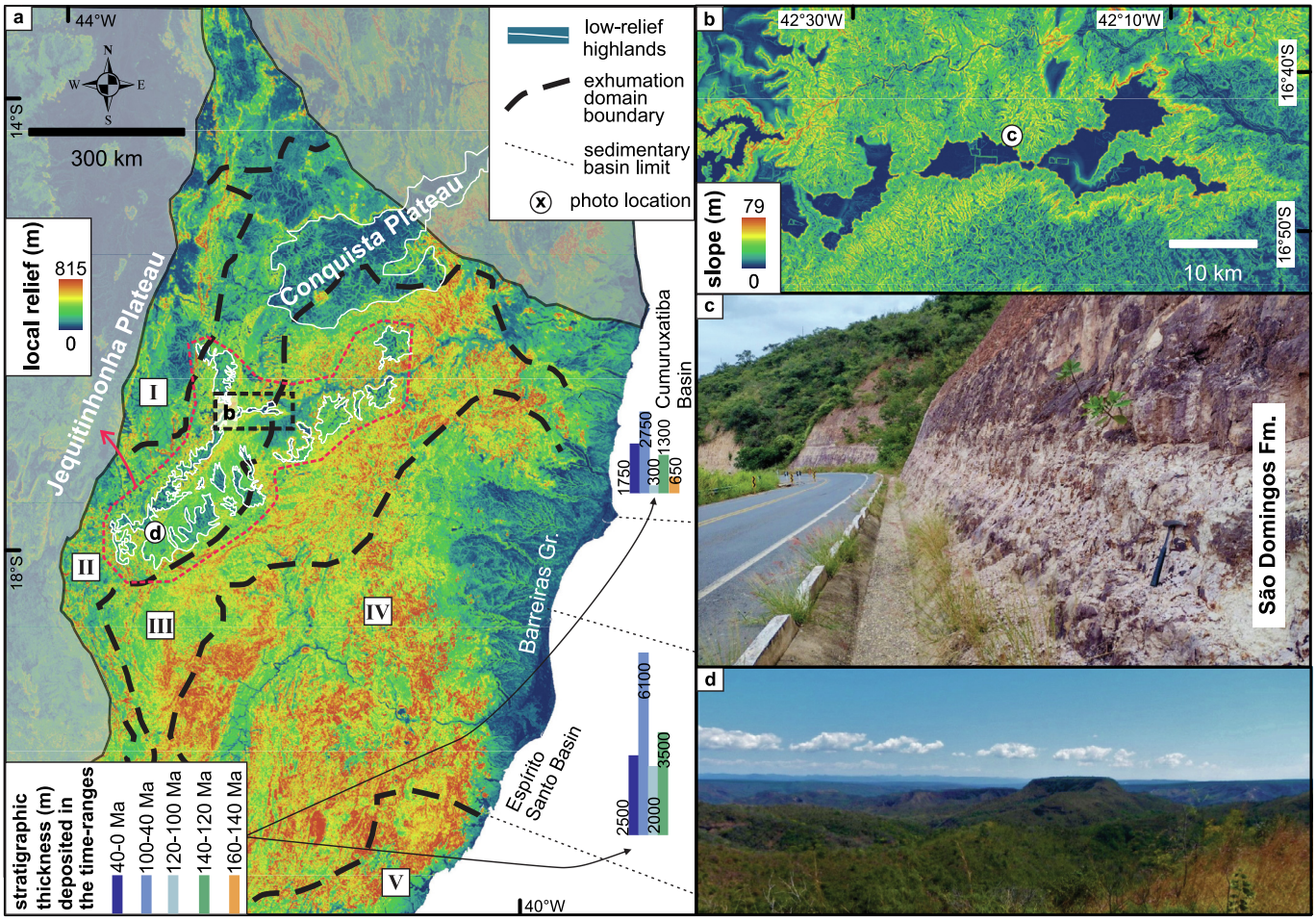

Fig. 6. (a) Map of local relief (range in elevation) of the Araçuaí Orogen considering a 500 m circular window. The main low-relief uplands of the Jequitinhonha and Conquista plateaus are highlighted. Estimates of sedimentary thickness for specific time intervals in the Cumuruxatiba and Espírito Santo basins from Milani (2007). (b) Zoom-in map of the low-relief upland area where photo (c) was taken (16°46′31.4″S, 42°22′34.1″E). (c) Deposits of São Domingos Formation (d) Landscape of the low-relief uplands in the Jequitinhonha Plateau, photo location indicated in (a)(17°52′10.6″S, 43°22′35.0″E).

II, and III) is likely to be more stable over geological time than the subduction-related zone in the south (Fig. 2; Domains IV and V) affected by repeated reactivations, such as in the Late Cretaceous – Paleocene cooling phase. Hence, the preservation of the Neogene São Domingos Formation and numerous elevated low-relief areas along the Jequitinhonha and Conquista plateaus, i.e., the so-called "chapadas" (Fig. 6; Valadão, 2009; Ferraz, 2020), attest to very low degrees of differential tectonic reactivations and erosion in Domains I, II and III. In contrast, such low-relief plateaus are absent in the characteristically high-relief areas of Domains IV and V, comprising, for example, the valleys of the Rio Doce and Mucuri rivers (see Fig. 6).

The magnitude of surface uplift and subsequent exhumation were likely also impacted by structural trends. In the northern part of the orogen, the structural fabric deviates to the NE, making it less parallel to the coastal margin and less able to respond to extensional forces conveyed by the opening and rifting of the South Atlantic (e.g., Salomon et al., 2017). For this reason, the coast of the Cumuruxatiba basin (Fig. 4), which is the closest to the SFC, appears to have experienced considerably less exhumation as a result of (post-)rift tectonics. In contrast, the younger AFT ages are concentrated in and along the dextral NE-oriented strike-slip shear zones to the south, principally in the Guaçu, Batatal, and Abre Campo zones (Fig. 2), which extend roughly parallel to the coast and up to the Ribeira Orogen. These areas appear to have been intensely reactivated and exhumed during the Mesozoic – Cenozoic, being cooled through the APAZ in the Late Cretaceous – Paleogene event (Fig. 5). The tectonic uplift (with erosional response) of the southern Araçuaí Orogen is probably associated with the Serra do Mar uplift and the formation of the Cenozoic Rift System of Southeastern Brazil (Fonte-Boa et al., 2022; Fig. 1).

Near the borders with the SFC, areas where the structural trend of the Proterozoic aulacogens (i.e., Pirapora and Paramirim) interacted with the Araçuaí Orogen (Domains II and III) show more rapid exhumation rates than those from other border zones between the SFC and the Araçuaí Orogen. For example, the Quadrilátero Ferrífero and the northern Espinhaço Range present slower cooling through the APAZ (Domain I). This is well-illustrated in the thermal history models of the Rio Pardo Salient at the Paramirim contact, where about 50 °C of rapid cooling during the Eocene to recent is documented (Figs. 2 and 4; Fonseca et al., 2022). The structure of the Rio Pardo Salient is thought to have resulted from the inversion of a deep master fault that is more likely to concentrate stress and localize vertical displacements under compressional stress fields (Bonini et al., 2012). The southern Espinhaço Range, close to Diamantina municipality, is located in the protrusion generated by the propagation of the deformation front into the Pirapora Aulacogen. Our findings suggest that this region of the Espinhaço Range is more susceptible to reactivation than the northern Espinhaço Range. This observation may explain why the southern Espinhaço Range is a high morphological drainage divide where the headwaters of tributaries of the Jequitinhonha and Doce rivers are located. The southern Espinhaço Range is composed of ridges and plateaus interspersed with intramontane depressions

and slopes of fluvial valleys in contrast to the northern portion, which is characterized by the widespread distribution of low-relief plateaus bordered by erosional ridges and scarps (Rezende and Salgado, 2011; Felippe et al., 2012).

The tectonic and structural fabric of the orogen decisively influences its erosion and denudation. Besides making reactivation easier, the weak zones of the structural framework determine areas susceptible to erosion, which is exploited, for example, by fluvial incision. For instance, Pedrosa-Soares et al. (2011) documented that the G5 plutonic bodies have distinct components, sizes, and properties according to the crustal levels exposed in the Araçuaí Orogen. Generally speaking, the crustal depth increases from north to south and from west to east, resulting in an apparent tendency for the exposure of smaller G5 bodies in the southern and eastern areas (Fig. 2; Temporim et al., 2021). These smaller G5 bodies represent roots of deeply eroded plutons, as opposed to the large G5 batholiths in the northern region, which delineate merged intrusions exposed in upper crustal levels. In addition, decreasing metamorphic grade (amphibolite to greenschist) and the presence of shallower sections of post-orogenic batholiths with significantly fewer mafic components are also signs that shallow crustal levels have been exposed in the northwestern region of the orogen (Trompette, 1994; Pedrosa-Soares et al., 2001, 2011). Crystallization pressures for these post-collisional intrusions were estimated between 2.4 and 3.5 kbar in the north and between 5.7 and 11.5 kbar in the south (Temporim et al., 2021). This suggests that the current exposure level represents a crustal section from paleodepths of about 10 km north and up to 35 km south. Therefore, the present study suggests that the Mesozoic – Cenozoic exhumation of the Araçuaí Orogen by differential erosion contributed in preserving the upper crust in the northern and western sectors.

5.3. Implications for adjacent passive margin basins

Mesozoic – Cenozoic exhumation events as constrained by low-temperature thermochronology in the Araçuaí Orogen undoubtedly impacted the development of adjacent passive margins basins. This is especially the case for the Espírito Santo, Mucuri, and Cumuruxatiba basins (Figs. 3 and 4). The spatial and chronological pattern of continental margin uplift and erosion aids in understanding the changes in sedimentary facies, burial history, and tectonic processes that also influence processes involved in oil and gas formation, accumulation, and their migration in these basins. Due to limited exploration drilling and other data from the Mucuri and Cumuruxatiba basins, many uncertainties remain with respect to the actual stratigraphy and, consequently, the presence of proper source-, reservoir- and seal rock facies, representing the most important elements of a petroleum system. Our discussions here will focus on more abundant data from the Espírito Santo Basin.

Our new AFT data and the data compilation presented in this paper suggest that the Mesozoic – Cenozoic tectonic activity and rate of basement denudation were strongly controlled by the proximity of the SFC, and partitioned in pre-existing shear zones (Fig. 5). The southern Araçuaí Orogen seems much more prone to tectonism than the northern coastal part of the orogen, which has been thermally more stable. Tectonic (in)stability can directly impact the prospecting for oil and gas (e.g., Nemčok, 2016), improving or diminishing a petroleum system's chances of becoming productive. Post-rift uplift of the underlying basement over which these basins developed can, for instance, increase the risk of seepage and expansion of the gas cap in the structure, presenting negative effects for hydrocarbon accumulation (Doré and Jensen, 1996; Ohm et al., 2008; Henriksen et al., 2011). Tectonic reactivations are responsible for the development of structural and stratigraphic traps, and, furthermore facilitate vertical migration along faults and accumulation in upper strata (Bryant et al., 2012).

In the southeastern Brazilian basins, post-salt turbidite reservoirs from the Urucutuca Formation, primarily oil-sourced from underlying *syn*-rift continental lacustrine rocks, are one of the main targets of petroleum exploration in the post-salt sequence. Frequent migration routes from source rocks in the pre-salt sequence to reservoirs in the post-salt are extensional listric faults and salt diapirs (Fig. 3), implying that some degree of tectonism appears to be advantageous for the post-salt petroleum systems in this area (Brun and Mauduit, 2008). Furthermore, the majority of the oil and gas resources off the coast are located in a segment of more frequent seismicity (e.g., Santos, Campos, and Espírito Santo basins; Assumpção, 1998; Borges et al., 2020), which may indicate that these 'productive' systems are associated with pieces of more reactive lithosphere. To the north, the proximity to the SFC has augmented the stability of the structures, which may have made it more difficult for hydrocarbons to migrate from the pre-salt source layers to the post-salt reservoirs.

Here we find that the magnitude of the Late Cretaceous – Paleocene erosion event differs across the Araçuaí Orogen. For instance, exhumation Domains IV and V, which are characterized by faster exhumation during that time, extend to large areas in the south but are limited to the north (Fig. 5). Therefore, an increase of sedimentary influx at that time can be expected from the north, i.e., Cumuruxatiba Basin, to the south, i.e., Espírito Santo Basin. Indeed, Upper Cenozoic slope strata in the Espírito Santo Basin comprise important reservoirs composed of prograding channel-fill deposits alternating with submarine fan deposits and blocky mass-transport deposits in the Urucutuca Formation (Alves, 2010; Gamboa et al., 2010). The sedimentary progradation loading generated evaporite remobilization and salt deformation in large salt diapirs, salt domes and anticlinal structures (Fig. 3). The growth of these salt structures played a key role in controlling the distribution of slope depocentres and the geometry of sand/reservoir-prone strata, as well as oil migration (Mohriak et al., 1995, 2012; Davison, 1999; Moraes et al., 2006; Alves and Cartwright, 2009; Fiduk and Rowan, 2012). For example, turtle structures filled with Late Cretaceous – Paleocene turbidities are considered deep-water prospects with high reserves potential (Fig. 3; e.g., Jubarte and Golfinho fields; Fiduk and Rowan, 2012). In this basin, oil and gas have been extracted since the 1970s, and the likelihood of additional discoveries is still thought to be high to moderate, particularly in sections closest to the coast, with exploration distributed in both pre- and post-salt sections (MME/EPE, 2012). Hence, it is suggested that episodes of increased sedimentation associated with halokinesis favored conditions for post-salt reservoir creation, migration, and entrapment of oil and gas in the Espírito Santo Basin.

In the Cumuruxatiba Basin, halokinetic deformation is likely principally triggered by the overload of the Abrolhos magmatic rocks from the late Paleocene to the Eocene (Ferreira et al., 2014). The salt structures in this basin are mainly represented by the formation of salt rollovers with just a few large salt diapirs (Ferreira et al., 2014). The differential halokinesis between the basins may be associated with the relative stability of the Cumuruxatiba Basin passive margin and its resulting lower sediment yield received during the Late Cretaceous – Paleocene phase (Jelinek et al., 2014). Accordingly, recommended exploration targets are primarily positioned in the Albian and pre-salt layers or the Eocene turbiditic sandstones, with low to intermediate chances of important discoveries (MME/EPE, 2012).

6. Conclusions

We present new apatite fission-track (AFT) data, considerably expanding the coverage of thermochronometric data for the Araçuaí Orogen. Furthermore, we present a compilation of the spa-

tial distribution of cooling ages and inverse thermal history models for the entire orogen based on this new data and incorporate available published datasets. We conclude the following:

(1) Rock cooling associated with erosional exhumation occurred during the Mesozoic – Cenozoic passive margin evolution of the Araçuaí Orogen, yet the rates varied spatially and temporally.

(2) Main phases of erosional exhumation and thus cooling to within the APAZ (~60 – 120 °C) include the (i) Jurassic – Hauterivian, associated with slow cooling and flexural subsidence of the Afro-Brazilian Depression; (ii) Barremian – Albian, linked with the erosion of the incipient Atlantic rift shoulders and the establishment of an oceanic base-level; and (iii) Late Cretaceous – Paleocene, related with post-rift reactivations that resulted in rapid cooling of the upper crust of the southeastern Araçuaí Orogen.

(3) Increasing proximity to the São Francisco Craton (SFC) coincides with slower denudation rates, suggesting that lithospheric stiffness exerts a first-order control on the magnitude of tectonic reactivation and associated surface uplift during the Mesozoic – Cenozoic.

(4) Inherited structures facilitated later reactivations. The structural framework of the Paramirim and Pirapora aulacogens, which controlled the geometry and structural evolution of the orogen border, is also associated with higher cooling rates during the Cretaceous compared to the rates at other parts of the orogen-craton boundary. Post-rift reactivation in the Late Cretaceous – Paleocene was controlled by the NE-oriented Guaçu, Batatal and Abre Campo shear zones.

(5) Mesozoic – Cenozoic differential exhumation contributes to the preservation of the upper crust in the northern and western sectors of the Araçuaí Orogen.

(6) The Late Cretaceous – Paleocene denudation phase produced sediment deposits that favored the deposition of vital oil and gas reservoirs in the Espírito Santo Basin. In addition, the loading of the prograding wedges promoted intense halokinesis that was imperative to the migration and entrapment of hydrocarbons in the post-salt section.

(7) In the Cumuruxatiba Basin, the relative tectonic stability and lower exhumation depths of the coastal area may have hampered the vertical migration of hydrocarbons and imposed a differential halokinesis.

CRediT authorship contribution statement

Ana Fonseca: Conceptualization, Methodology, Formal analysis, Investigation, Writing – original draft, Visualization. **Tiago Novo:** Conceptualization, Funding acquisition, Resources, Writing – review & editing. **Tobias Fonte-Boa:** Conceptualization, Writing – review & editing. **Matheus Kuchenbecker:** Conceptualization, Resources, Writing – review & editing. **Daniel Galvão Carnier Fragoso:** Conceptualization, Writing – review & editing. **Daniel Peifer:** Conceptualization, Writing – review & editing. **Antônio Carlos Pedrosa-Soares:** Conceptualization, Writing – review & editing. **Johan De Grave:** Conceptualization, Methodology, Validation, Formal analysis, Investigation, Resources, Writing – review & editing, Supervision.

Declaration of Competing Interest

The authors declare that they have no known competing financial interests or personal relationships that could have appeared to influence the work reported in this paper.

Acknowledgements

We acknowledge CAPES-Brazil (CAPESPrint 88887.371253/2019-00) for financial support (JDG) during the field work. M.K. is a fellow of the Brazilian Research Council – CNPq (#314667/2021-0) and appreciates the support.

Appendix A. Supplementary data

Supporting images, graphs, and tables of the Apatite Fission Track data. Supplementary data to this article can be found online at https://doi.org/10.1016/j.gsf.2023.101628.

References

Alkmim, F.F., Kuchenbecker, M., Reis, H.L.S., Pedrosa-Soares, A.C., 2017. The Araçuaí Belt. In: Heilbron, M., Cordani, U.G., Alkmim, F.F. (Eds.), São Francisco Craton, Eastern Brazil. Springer, pp. 255–275. https://doi.org/10.1007/978-3-319-01715-0.

Alkmim, F.F., Marshak, S., Pedrosa-Soares, A.C., Peres, G.G., Cruz, S.C.P., Whittington, A., 2006. Kinematic evolution of the Araçuaí-West Congo orogen in Brazil and Africa: Nutcracker tectonics during the Neoproterozoic assembly of Gondwana. Precambrian Res. 149, 43–64. https://doi.org/10.1016/j.precamres.2006.06.007.

Allen, P.A., Armitage, J.J., 2012. Cratonic basins. In: Busby, C., Azor, A. (Eds.), Tectonics of Sedimentary Basins: Recent Advances. Blackwell Publishing Ltd., Published, pp. 602–620.

Alves, T.M., 2010. 3D Seismic examples of differential compaction in mass-transport deposits and their effect on post-failure strata. Mar. Geol. 271, 212–224. https://doi.org/10.1016/j.margeo.2010.02.014.

Alves, T.M., Cartwright, J.A., 2009. Volume balance of a submarine landslide in the Espírito Santo Basin, offshore Brazil: quantifying seafloor erosion, sediment accumulation and depletion. Earth Planet. Sci. Lett. 288, 572–580. https://doi.org/10.1016/j.epsl.2009.10.020.

Amaral, L., Caxito, F.A., Pedrosa-Soares, A., Queiroga, G., Babinski, M., Trindade, R., Lana, C., Chemale, F., 2020. The Ribeirão da Folha ophiolite-bearing accretionary wedge (Araçuaí orogen, SE Brazil): New data for Cryogenian plagiogranite and metasedimentary rocks. Precambrian Res. 336, 105522.

Amaral Santos, E., Jelinek, A.R., Machado, J.P., Stockli, D., 2022. Thermal history along the Araçuaí Orogen and São Francisco Craton border, eastern Brazilian continental margin, based on low-temperature thermochronologic data. Tectonophysics 825, 229232. https://doi.org/10.1016/j.tecto.2022.229232.

Amaral-Santos, E., Jelinek, A.R., Genezine, F.A., 2019. Phanerozoic cooling history of Archean/Paleoproterozoic basement in the southern Espinhaço Range, southeastern Brazil, through apatite fission-track analysis. J. South Am. Earth Sci. 96, 102352. https://doi.org/10.1016/j.jsames.2019.102352.

Ashby, D., Mccaffrey, K., Holdsworth, B., Almeida, J., 2010. Structural Controls on the Evolution of the Southeastern Brazilian Continental Margin, in: Geophysical Research Abstracts. EGU General Assembly.

Assumpção, M., 1998. Focal mechanisms of small earthquakes in the southeastern Brazilian shield: A test of stress models of the South American plate. Geophys. J. Int. 133, 490–498. https://doi.org/10.1046/j.1365-246x.1998.00532.x.

Babinski, M., Pedrosa-Soares, A.C., Trindade, R.I.F., Martins, M., Noce, C.M., Liu, D., 2012. Neoproterozoic glacial deposits from the Araçuaí orogen, Brazil: Age, provenance and correlations with the São Francisco craton and West Congo belt. Gondwana Res. 21, 451–465. https://doi.org/10.1016/j.gr.2011.04.008.

Barrote, V.R., Volante, S., Blereau, E.R., Rosière, C.A., Spencer, C.J., 2022. Implications of the dominant LP–HT deformation in the Guanhães Block for the Araçuaí West-Congo Orogen evolution. Gondwana Res. 107, 154–175. https://doi.org/10.1016/j.gr.2022.03.012.

Batezelli, A., Ladeira, F.S.B., 2016. Stratigraphic framework and evolution of the Cretaceous continental sequences of the Bauru, Sanfranciscana, and Parecis basins, Brazil. J. South Am. Earth Sci. 65, 1–24. https://doi.org/10.1016/j.jsames.2015.11.005.

Bertolini, G., Marques, J.C., Hartley, A.J., Basei, M.A.S., Frantz, J.C., Santos, P.R., 2021. Determining sediment provenance history in a Gondwanan erg: Botucatu formation, Northern Paraná Basin, Brazil. Sediment. Geol. 417, 105883. https://doi.org/10.1016/j.sedgeo.2021.105883.

Bertotti, A.L., Chemale, F., Sylvester, P.J., Kayser, V.T., Gruber, L., 2014. Changing provenance of Late Jurassic to Early Cretaceous rift-related sedimentary rocks of the South Atlantic Margin: LA-MC-ICPMS U-Pb and Lu–Hf isotopic study of detrital zircons from the Camamu Basin, Eastern Brazil. Chem. Geol. 363, 250–261. https://doi.org/10.1016/j.chemgeo.2013.10.030.

Bishop, P., 2007. Long-term landscape evolution: linking tectonics and surface processes. Earth Surf. Process. Landforms 32, 329–365. https://doi.org/10.1002/esp.1493.

Bonini, M., Sani, F., Antonielli, B., 2012. Basin inversion and contractional reactivation of inherited normal faults: A review based on previous and new experimental models. Tectonophysics 522–523, 55–88. https://doi.org/10.1016/j.tecto.2011.11.014.

Borges, R.G., Assumpção, M.S., Almeida, M.C.F., de Almeida, M., S.S. de, 2020. Seismicity and seismic hazard in the continental margin of southeastern Brazil. J. Seismol. 24, 1205–1224. https://doi.org/10.1007/s10950-020-09941-4.
Braun, J., van der Beek, P., Batt, G., 2006. Quantitative Thermochronology: Numerical Methods for the Interpretation of Thermochronological Data. Cambridge University Press, New York, p. 272.
Brown, R.W., Gallagher, K., Johnson, K., Cockburn, H.A., Summerfield, M.A., Gleadow, A.J.W., 2001. All landscapes, great and small: problems and strategies for deriving regional denudation histories from sparse data. Earth System Processes, Abst. Geol. Soc. Amer. and Geol. Soc. Lond., Edinburgh, Scotland, 81.
Brun, J.P., Mauduit, T.P.O., 2008. Rollovers in salt tectonics: the inadequacy of the listric fault model. Tectonophysics 457, 1–11. https://doi.org/10.1016/j.tecto.2007.11.038.
Bryant, I., Herbst, N., Dailly, P., Dribus, J.R., Fainstein, R., Harvey, N., McCoss, A., Montaron, B., Quirk, D., Tapponnier, P., 2012. Basin to basin: Plate tectonics in exploration. Oilfield Review 24 (3), 38–57.
Cainelli, C., Mohriak, W.U., 1999. Some remarks on the evolution of sedimentary basins along the eastern Brazilian continental margin. Episodes 22, 206–216. https://doi.org/10.18814/epiiugs/1999/v22i3/008.
Caixeta, J.M., Milhomem, O.S., Witzke, R.E., Dupuy, I.S.S., Gontijo, G.A., 2007. Bacia de Camamu. Bol. Geociênc. Petrobrás 15 (2), 455–461 (in Portuguese).
Carmo, I.O., 2005. Geocronologia do intemperismo Cenozóico no sudeste do Brasil. PhD thesis. Federal Univ. Rio de Janeiro (Brazil) (in Portuguese).
Caxito, F.A., Hartmann, L.A., Heilbron, M., Pedrosa-Soares, A.C., Bruno, H., Basei, M.A. S., Chemale, F., 2022. Multi-proxy evidence for subduction of the Neoproterozoic Adamastor Ocean and Wilson cycle tectonics in the South Atlantic Brasiliano Orogenic System of Western Gondwana. Precambrian Res. 376, 106678. https://doi.org/10.1016/j.precamres.2022.106678.
Cesero, P., Ponte, F.C., 1972. Análise comparativa da paleogeologia dos litorais atlânticos brasileiro e africano. Boletim de Geociências da PETROBRAS 11 (1), 1–18 (in Portuguese).
Chang, H.K., Kowsmann, R.O., Figueiredo, A.M.F., Bender, A., 1992. Tectonics and stratigraphy of the East Brazil Rift system: an overview. Tectonophysics 213, 97–138. https://doi.org/10.1016/0040-1951(92)90253-3.
Chemale Jr., F., Dussin, I.A., Alkmim, F.F., Martins, M.S., Queiroga, G., Armstrong, R., Santos, M.N., 2012. Unravelling a Proterozoic basin history through detrital zircon geochronology: The case of the Espinhaço Supergroup, Minas Gerais, Brazil. Gondwana Res. 22, 200–206. https://doi.org/10.1016/j.gr.2011.08.016.
Coelho, R.M., Chaves, A.O., 2017. Diques máficos de Minas Gerais do Cretáceo Inferior: Idades Ar-Ar e correlação com a Província Ígnea Paraná-Etendeka. Geociências 4, 613–622 (in Portuguese).
Cogné, N., Gallagher, K., Cobbold, P.R., 2011. Post-rift reactivation of the onshore margin of southeast Brazil: evidence from apatite (U-Th)/He and fission-track data. Earth Planet. Sci. Lett. 309, 118–130. https://doi.org/10.1016/j.epsl.2011.06.025.
Cogné, N., Gallagher, K., Cobbold, P.R., Riccomini, C., Gautheron, C., 2012. Post-breakup tectonics in southeast Brazil from thermochronological data and combined inverse-forward thermal history modeling. J. Geophys. Res. 117, 1–16. https://doi.org/10.1029/2012JB009340.
Contreras, J., Zühlke, R., Bowman, S., Bechstädt, T., 2010. Seismic stratigraphy and subsidence analysis of the southern Brazilian margin (Campos, Santos and Pelotas basins). Mar. Pet. Geol. 27, 1952–1980. https://doi.org/10.1016/j.marpetgeo.2010.06.007.
Costa, A.F. de O., Danderfer, A., Bersan, S.M., 2018b. Record of a Statherian rift-sag basin in the Central Espinhaço Range: Facies characterization and geochronology. J. South Am. Earth Sci. 82, 311–328. https://doi.org/10.1016/j.jsames.2017.10.014.
Craddock, J.P., Malone, D.H., Porter, R., Compton, J., Luczaj, J., Konstantinou, A., Day, J.E., Johnston, S.T., 2017. Paleozoic reactivation structures in the Appalachian-Ouachita-Marathon foreland: Far-field deformation across Pangea. Earth-Sci. Rev. 169, 1–34. https://doi.org/10.1016/j.earscirev.2017.04.002.
Cruz, S.C.P., Alkmim, F.F., 2006. The tectonic interaction between the Paramirim aulacogen and the Araçuaí belt, São Francisco craton region, Eastern Brazil. An. Acad. Bras. Cienc. 78, 151–173. https://doi.org/10.1590/s0001-37652006000100014.
Cruz, S.C.P., Alkmim, F.F., Barbosa, J.S.F., Dussin, I., Gomes, L.C.C., 2015. Tectonic inversion of compressional structures in the southern portion of the Paramirim corridor, Bahia, Brazil. Brazil. J. Geol. 45, 541–567. https://doi.org/10.1590/2317-488920150030240.
Cruz, S.C.P., Alkmim, F.F., 2017. The Paramirim Aulacogen. In: Heilbron, M., Cordani, U.G., Alkmim, F.F. (Eds.), São Francisco Craton. Springer International Publishing Switzerland, Eastern Brazil, pp. 97–115. https://doi.org/10.1007/978-3-319-01715-0_6.
Cunningham, D., Alkmim, F.F., Marshak, S., 1998. A structural transect across the coastal mobile belt in the Brazilian Highlands (latitude 20°S): the roots of a Precambrian transpressional orogen. Precambrian Res. 92, 251–275. https://doi.org/10.1016/S0301-9268(98)00077-1.
Cunningham, D., Earth, E., Connecticut, E., States, U., 2021. Tectonic Geomorphology of Intracontinental Mountain Ranges, 2nd ed., Treatise on Geomorphology. Elsevier Inc. https://doi.org/10.1016/B978-0-12-818234-5.00091-2.
Davison, I., 1999. Tectonics and hydrocarbon distribution along the Brazilian South Atlantic margin. Geol. Soc. London. Spec. Publ. 153, 133–151. https://doi.org/10.1144/GSL.SP.1999.153.01.09.
Almeida, F.F.M. de, Carneiro, C.D.R., Mizusaki, A.M.P., 1996. Correlação do magmatismo das bacias da margem continental brasileira com o das áreas emersas adjacentes. Rev. Bras. Geociências 26, 125–138 (in Portuguese). https://doi.org/10.25249/0375-7536.19963125138.
Almeida, F.F.M. de., 1961. Petrologia da Ilha da Trindade (Provimento de Cátedra). Universidade de São Paulo, São Paulo (in Portuguese).
De Corte, F., Bellemans, F., Van den Haute, P., Ingelbrecht, C., Nicholl, C., 1998. A new U doped glass certified by the european commission for the calibration of fission- track dating. In: Van den haute, P., De Corte, F. (Eds.), Advances in Fission-track Geochronology. Kluwer Academic Publishers, Dordrecht, pp. 67–78.
de Costa, A.F.O., Danderfer, A., Lana, C., 2018a. Stratigraphic and geochronological characterization of the Mato Verde group, Central Espinhaço (Brazil): an Eocalymmian rifting record in the western domain of the Congo-São Francisco paleocontinent. J. South Am. Earth Sci. 84, 16–33. https://doi.org/10.1016/j.jsames.2018.03.005.
De Grave, J., Glorie, S., Vermaercke, P., Vittiglio, G., 2010. A 'new' irradiation facility for FT applications at the Belgian nuclear research centre: the BR1 reactor. In: 12th International Conference on Thermochronology (Thermo 2010).
de Oliveira, C.H.E., Jelinek, A.R., Chemale, F., Bernet, M., 2016. Evidence of post-Gondwana breakup in Southern Brazilian Shield: insights from apatite and zircon fission track thermochronology. Tectonophysics 666, 173–187. https://doi.org/10.1016/j.tecto.2015.11.005.
Degler, R., Pedrosa-Soares, A., Dussin, I., Queiroga, G., Schulz, B., 2017. Contrasting provenance and timing of metamorphism from paragneisses of the Araçuaí-Ribeira orogenic system, Brazil: Hints for Western Gondwana assembly. Gondwana Res. 51, 30–50. https://doi.org/10.1016/j.gr.2017.07.004.
Degler, R., Pedrosa-Soares, A., Novo, T., Tedeschi, M., Silva, L.C., Dussin, I., Lana, C., 2018. Rhyacian-Orosirian isotopic records from the basement of the Araçuaí-Ribeira orogenic system (SE Brazil): links in the Congo-São Francisco palaeocontinent. Precambrian Res. 317, 179–195.
Donelick, R.A., 1991. Crystallographic orientation dependence of mean etchable fission track length in apatite: an empirical model and experimental observations. Am. Mineral. 76, 83–91.
Donelick, R.A., 1993. Apatite etching characteristics versus chemical composition. Nucl. Tracks Radiat. Meas. 21, 604.
Donelick, R.A., Ketcham, R.A., Carlson, W.D., 1999. Variability of apatite fission-track annealing kinetics: II. Crystallographic orientation effects. Am. Mineral. 84, 1224–1234. https://doi.org/10.2138/am-1999-0902.
Doré, A.G., Jensen, L.N., 1996. The impact of late Cenozoic uplift and erosion on hydrocarbon exploration; offshore Norway and some other uplifted basins. Glob. Planet. Change 12, 415–436.
Dussin, I.A., Dussin, T.M., 1995. O Supergrupo Espinhaço: Modelo de evolução geodinâmica. Geonomos 1, 19–26 (in Portuguese).
Felippe, M.F., Silva, C.A., Souza, A.H., Magalhães Júnior, A.P., 2012. Caracterização Morfométrica dos Compartimentos do Relevo do Parque Nacional da Serra do Cipó, Serra do Espinhaço Meridional— Minas Gerais. Revista Espinhaço 1, 3–14 (in Portuguese).
Fernandes, L.A., Magalhães Ribeiro, C.M., 2015. Evolution and palaeoenvironment of the Bauru Basin (Upper Cretaceous, Brazil). J. South Am. Earth Sci. 61, 71–90. https://doi.org/10.1016/j.jsames.2014.11.007.
Ferraz, C.M.L., 2020. Isostasia flexural adjacente à margem continental passiva brasileira: das "chapadas" do Jequitinhonha à planície costeira do sul da Bahia. Vozes dos Val. 17 (in Portuguese).
Ferreira, T.S., de Araújo, M.N.C., Alves da Silva, F.C., 2014. Cenozoic folding in the Cumuruxatiba basin, Brazil: An approach to the deformation trigger by the Abrolhos magmatism. Mar. Pet. Geol. 54, 47–64. https://doi.org/10.1016/j.marpetgeo.2014.02.012.
Ferreira, T.S., 2010. Análise estrutural da deformação Cenozóica na Bacia de Cumuruxatiba (BA). Master's thesis, Federal Univ. Rio Grande do Norte (Brazil), 127p (in Portuguese).
Fiduk, C.J., Rowan, M.G., 2012. Analysis of folding and deformation within layered evaporites in Blocks BM-S-8 & -9, Santos Basin, Brazil. In: Alsop, G. I., Archer, S. G., Hartley, A. J., Grant, N.T., Hodgkinson, R. (Eds.), Salt Tectonics, Sediments and Prospectivity. Geological Society, London, Special Publications, 363, 471–487.
Figueiredo, A.M.F., Braga, J.A.E., Zabalaga, J.C., Oliveira, J.J., Aguiar, G.A., Silva, O.B., Mato, L.F., Daniel, L.M.F., Magnavita, L.P., Bruhn, C.H.L., 1994. Recôncavo basin, Brazil: A prolific intracontinental rift basin: AAPG Memoir 59, pp. 157–203.
Flament, N., Gurnis, M., Dietmar Müller, R., 2013. A review of observations and models of dynamic topography. Lithosphere 5, 189–210. https://doi.org/10.1130/L245.1.
Fleck, J.B.F., 2014. Geoquímica, Geocronologia e Contexto Geotectônico do Magmatismo Máfico Associado ao Feixe de Fraturas Colatina, Estado Espirito Santo. Federal Univ.. PhD Thesis.Minas Gerais (Brazil), 134p (in Portuguese).
Fleischer, R.L., Price, P.B., Walker, R.M., 1975. Nuclear Tracks in Solids: Principles and Applications. Univ of California Press.
Fonseca, A., Cruz, S., Novo, T., He, Z., Grave, J.D., 2022. Differential exhumation of cratonic and non - cratonic lithosphere revealed by apatite fission – track thermochronology along the edge of the São Francisco craton, eastern Brazil. Sci. Rep. 1–9. https://doi.org/10.1038/s41598-022-06419-w.
Fonseca, A.C.L., Novo, T.A., Nachtergaele, S., Fonte-Boa, T.M.R., Van Ranst, G., De Grave, J., 2021. Differential Phanerozoic evolution of cratonic and non-cratonic lithosphere from a thermochronological perspective: São Francisco Craton and marginal orogens (Brazil). Gondwana Res. 93, 106–126. https://doi.org/10.1016/j.gr.2021.01.006.
Fonseca, A.C., Piffer, G.V., Nachtergaele, S., Van Ranst, G., De Grave, J., Novo, T.A., 2020. Devonian to Permian post-orogenic denudation of the Brasília Belt of

West Gondwana: insights from apatite fission track thermochronology. J. Geodyn. 137, 101733. https://doi.org/10.1016/j.jog.2020.101733.
Fonte-boa, T.M.R., Peifer, D., Fonseca, A., Novo, T.A., 2022. The southeast Brazilian rifted continental margin is not a single, continuous upwarp : variations in morphology and denudation patterns along the continental drainage divide. Earth-Science Rev. 231, 104091. https://doi.org/10.1016/j.earscirev.2022.104091.
França, R.L., Del Rey, A.C., Tagliari, C.V., Brandão, J.R., Fontanelli, P.R., 2007b. Bacia do Mucuri. Boletim de Geociências da Petrobras 15 (2), 493–499. in Portuguese.
França, R.L., Ragagnin, G.M., 1996. A influência do vulcanismo de abrolhos na sedimentação terciária da Bacia de Mucuri. Congr. Bras. Geol 39 (5), 431–432 (in Portuguese).
França, R.L., Del Rey, A.C., Tagliari, C.V., Brandão, J.R., Fontanelli, P.D.R., 2007a. Bacia do Espírito Santo. Boletim de Geociências da Petrobras 15 (2), 501–509. in Portuguese.
Franco-Magalhaes, A.O.B., Hackspacher, P.C., Glasmacher, U.A., Saad, A.R., 2010. Rift to post-rift evolution of a "passive" continental margin: The Ponta Grossa Arch. SE Brazil. Int. J. Earth Sci. 99, 1599–1613. https://doi.org/10.1007/s00531-010-0556-8.
Franco-Magalhaes, A.O.B., Cuglieri, M.A.A., Hackspacher, P.C., Saad, A.R., 2014. Long-term landscape evolution and post-rift reactivation in the southeastern Brazilian passive continental margin: Taubaté basin. Int. J. Earth Sci. 103, 441–453. https://doi.org/10.1007/s00531-013-0967-4.
Galbraith, R.F., 2005. Statistics for Fission Track Analysis. Chapman and Hall/CRC, New York.
Gallagher, K., 2012. Transdimensional inverse thermal history modeling for quantitative thermochronology. J. Geophys. Res.: Solid Earth 117 (B2), B02408. https://doi.org/10.1029/2011JB008825.
Gallagher, K., Hawkesworth, C.J., Mantovani, M.S.M., 1994. The denudation history of the offshore continental margin of SE Brazil inferred from apatite fission-track data. J. Geophys. Res. 99, 18117–18145.
Gallagher, K., Stephenson, J., Brown, R.W., Holmes, C., Ballester, P., 2005. Exploiting 3D spatial sampling in inverse modeling of thermochronological data. Rev. Mineral. Geochem. 58 (1), 375–387. https://doi.org/10.2138/rmg.2005.58.14.
Gamboa, D., Alves, T., Cartwright, J., Terrinha, P., 2010. MTD distribution on a "passive" continental margin: the Espírito Santo Basin (SE Brazil) during the Palaeogene. Mar. Pet. Geol. 27, 1311–1324. https://doi.org/10.1016/j.marpetgeo.2010.05.008.
Garcia, A.J.V., da Rosa, A.S., Goldberg, K., 2005. Paleoenvironmental and paleoclimatic control on early diagenetic processes and fossil record in Cretaceous continental sandstones of Brazil. J. S. Am. Earth. Sci. 19, 243–258.
Geraldes, M.C., Motoki, A., Costa, A., Mota, C.E., Mohriak, W.U., 2013. Geochronology (Ar/Ar and K-Ar) of the South Atlantic post-break-up magmatism. In: Mohriak, W.U., Danforth, A., Post, P.J., Brown, D.E., Tari, G.C., Nemčok, M., Sinha, S.T. (Eds.), Conjugate Divergent Margins. Geological Society Special Publication, pp. 41–74. https://doi.org/10.1144/SP369.21.
Ghignone, J.I., 1979. Geologia dos sedimentos fanerozóicos do Estado da Bahia. Geologia e recursos minerais do Estado da Bahia: textos básicos, 1 (in Portuguese).
Gilchrist, A.R., Summerfield, M.A., 1990. Differential denudation and flexural isostasy in formation of rifted-margin upwarps. Nature 346 (6286), 739.
Gilchrist, A.R., Summerfield, M.A., Cockburn, H.A.P., 1994. Landscape dissection, isostatic uplift, and the morphologic development of orogens. Geology 22 (11), 963–966.
Gleadow, A.J.W., Brown, R.W., 2000. Fission track thermochronology and the long-term denudational response to tectonics. In: Summerfield, M.J. (Ed.), Geomorphology and Global Tectonics. Wiley, New York, pp. 57–75.
Gleadow, A.J.W., Duddy, I.R., Green, P.F., Lovering, J.F., 1986. Confined track lengths in apatite—A diagnostic tool for thermal history analysis. Contrib. Mineral. Petrol. 94, 405–415.
Green, P.F., Duddy, I.R., Laslett, G.M., Hegarty, K.A., Gleadow, A.J.W., Lovering, J.F., 1989. Thermal annealing of fission tracks in apatite 4. Quantitative modelling techniques and extension to geological timescales. Chem. Geol. Isot. Geosci. Sect. 79, 155–182. https://doi.org/10.1016/0168-9622(89)90018-3.
Grochowski, J., Kuchenbecker, M., Barbuena, D., Novo, T., 2021. Disclosing Rhyacian/Orosirian orogenic magmatism within the Guanhães basement inlier, Araçuaí Orogen, Brazil: A new piece on the assembly of the São Francisco-Congo paleocontinent. Precambrian Res. 363, 106329. https://doi.org/10.1016/j.precamres.2021.106329.
Guadagnin, F., Chemale, F., Magalhães, A.J.C., Santana, A., Dussin, I., Takehara, L., 2015. Age constraints on crystal-tuff from the Espinhaço Supergroup — Insight into the Paleoproterozoic to Mesoproterozoic intracratonic basin cycles of the Congo-São Francisco Craton. Gondwana Res. 27, 363–376. https://doi.org/10.1016/j.gr.2013.10.009.
Hackspacher, P.C., Ribeiro, L.F.B., Ribeiro, M.C.S., Fetter, A.H., Hadler Neto, J.C., Tello, C.E.S., Dantas, E.L., 2004. Consolidation and break-up of the South American Platform in southeastern Brazil: Tectonothermal and denudation histories. Gondwana Res. 7, 91–101. https://doi.org/10.1016/S1342-937X(05)70308-7.
Heilbron, M., Mohriak, W., Valeriano, C. M., Milani, E., Almeida, J.C. A., Tupinambá, M., 2000. From collision to extension: the roots of the southeastern continental margin of Brazil. In: Mohriak, W., Talwani, M. (Eds.), Atlantic Rifts and Continental Margins. American Geophysical Union, Geophysical Monograph, 115, pp. 1–32.
Heine, C., Zoethout, J., Müller, R.D., 2013. Kinematics of the South Atlantic rift. Solid Earth 4, 215–253. https://doi.org/10.5194/se-4-215-2013.
Henriksen, E., Ryseth, A.E., Larssen, G.B., Heide, T., Ronning, K., Sollid, K., Stoupakova, A.V., 2011. Chapter 10: Tectonostratigraphy of the greater Barents Sea: implications for petroleumsystems. In: Spencer, A.M., Embry, A.F., Gautier, D. L., Stoupakova, A.V., Soensen, K. (Eds.), Arctic Petroleum Geology. Geological Society, London, Memoirs, 35, pp. 163–195.
Henry, S.G., Brumbaugh, W., 1995. Pre-Salt Rock Development on Brazil's Conjugate Margin: West African Examples. 4th International Congress of the Brazilian Geophysical Society, Rio de Janeiro, Expanded Abstracts, I, pp. 68–70.
Hiruma, S.T., Riccomini, C., Modenesi-Gauttieri, M.C., Hackspacher, P.C., Hadler Neto, J.C., Franco-Magalhães, A.O.B., 2010. Denudation history of the Bocaina Plateau, Serra do Mar, southeastern Brazil: relationships to Gondwana breakup and passive margin development. Gondwana Res. 18, 674–687. https://doi.org/10.1016/j.gr.2010.03.001.
Hurford, A.J., Green, P.F., 1982. A users' guide to fission track dating calibration. Earth Planet. Sci. Lett. 59, 343–354. https://doi.org/10.1016/0012-821X(82)90136-4.
Hurford, A.J., Green, P.F., 1983. The zeta age calibration of fission-track dating. Isot. Geosci. 1, 285–317. https://doi.org/10.1016/S0009-2541(83)80026-6.
Jelinek, A.R., Chemale, F., van der Beek, P.A., Guadagnin, F., Cupertino, J.A., Viana, A., 2014. Denudation history and landscape evolution of the northern East-Brazilian continental margin from apatite fission-track thermochronology. J. South Am. Earth Sci. 54, 158–181. https://doi.org/10.1016/j.jsames.2014.06.001.
Ketcham, R.A., 2005. Forward and inverse modeling of low-temperature thermochronometry data. Rev. Mineral. Geochemistry 58, 275–314. https://doi.org/10.2138/rmg.2005.58.11.
Ketcham, R.A., Carter, A., Donelick, R.A., Barbarand, J., Hurford, A.J., 2007. Improved measurement of fission-track annealing in apatite using *c*-axis projection. Am. Mineral. 92, 789–798. https://doi.org/10.2138/am.2007.2280.
Kohn, B.P., 2005. Visualizing thermotectonic and denudation histories using apatite fission track thermochronology. Rev. Mineral. Geochem. 58, 527–565. https://doi.org/10.2138/rmg.2005.58.20.
Kuchenbecker, M., Pedrosa-Soares, A.C., Babinski, M., Fanning, M., 2015. Detrital zircon age patterns and provenance assessment for pre-glacial to post-glacial successions of the Neoproterozoic Macaúbas Group, Araçuaí orogeny, Brazil. Precambrian Res. 266, 12–26. https://doi.org/10.1016/j.precamres.2015.04.016.
Kuchenbecker, M., Pedrosa-Soares, A.C., Babinski, M., Reis, H.L.S., Atman, D., da Costa, R.D., 2020. Towards an integrated tectonic model for the interaction between the Bambuí basin and the adjoining orogenic belts: Evidences from the detrital zircon record of syn-orogenic units. J. South Am. Earth Sci. 104, 102831. https://doi.org/10.1016/j.jsames.2020.102831.
Kuchle, J., Scherer, C.M.S., Born, C.C., Alvarenga, R.S., Adegas, F., 2011. A contribution to regional stratigraphic correlations of the Afro-Brazilian depression - The Dom João Stage (Brotas Group and equivalent units - Late Jurassic) in North- eastern Brazilian sedimentary basins. J. S. Am. Earth. Sci. 31, 358–371.
Laslett, G.M., Green, P.F., Duddy, I.R., Gleadow, A.J.W., 1987. Thermal annealing of fission tracks in apatite. 2. A quantitative analysis. Chem. Geol. (Isotopes Geoscience Section) 65, 1–13.
Lucazeau, F., 2019. Analysis and mapping of an updated terrestrial heat flow data set. Geochemistry. Geophys. Geosyst. 20, 4001–4024. https://doi.org/10.1029/2019GC008389.
Macgregor, D.S., 2020. Regional variations in geothermal gradient and heat flow across the African plate. J. African Earth Sci. 171, 103950. https://doi.org/10.1016/j.jafrearsci.2020.103950.
Magnavita, L.P., 1992. Geometry and Kinematics of the Reconcavo-Tucano-Jatoba Rift, NE Brazil. Ph.D. thesis. University of Oxford (England).
Malusà, M.G., Fitzgerald, P.G., 2019. From cooling to exhumation: setting the reference frame for the interpretation of thermochronologic data. In: Malusà, M. G., Fitzgerald, P.G. (Eds.), Fission-track Thermochronology and Its Application to Geology. Springer, Cham, pp. 147–164.
Menegazzo, M.C., Catuneanu, O., Chang, H.K., 2016. The South American retroarc foreland system: The development of the Bauru Basin in the back-bulge province. Mar. Pet. Geol. 73, 131–156. https://doi.org/10.1016/j.marpetgeo.2016.02.027.
Milani, E.J., 2007. Bacias sedimentares brasileiras: cartas estratigráficas. Boletim de Geociências da PETROBRAS 15 (2), 183–205.
MME, EPE, 2012. Zoneamento Nacional de Recursos de Óleo e Gás, 2012. Ministério de Minas e Energia. Empresa de Pesquisa Energética, Brasília (in Portuguese).
Modica, C.J., Brush, E.R., 2004. Postrift sequence stratigraphy, paleogeography, and fill history of the deep-water Santos Basin, offshore southeast Brazil. AAPG (Am. Assoc. Pet. Geol.) Bull. 88, 923–945.
Mohriak, W.U., 2003. Bacias sedimentares da margem continental Brasileira. In: Bizzi, L.A., Schobbenhaus, C., Vidotti, C., Goncalves, J.H. (Eds.), Geologia, Tectonica e Recursos Minerais Do Brasil. CPRM, Brasilia, pp. 87–165 (in Portuguese).
Mohriak, W.U., Macedo, J.M., Castellani, R.T., Rangel, H.D., Barros, A.Z.N., Latgé, M.A. L., Ricci, J.A., Misuzaki, A.M.P., Szatmari, P., Demercian, L.S., Rizzo, J.G., Aires, J.R., 1995. Salt tectonics and structural styles in the deep-water province of the Cabo Frio region, Rio de Janeiro, Brazil. In: Jackson, M.P.A., Roberts, D.G., Snelson, S. (Eds.), Salt Tectonics: A Global Perspective. AAPG Memoir, Vol. 65, pp. 273–304.
Mohriak, W., Nemcok, M., Enciso, G., 2008. South Atlantic divergent margin evolution: rift-border uplift and salt tectonics in the basins of SE Brazil. In: Pankhurst, R.J., Trouw, R.A.J., Brito Neves, B.B., De Wit, M.J. (Eds.), West Gondwana: Pre-Cenozoic Correlations Across the South Atlantic Region. Geol. Soc. Spec. Publ, Vol. 294, pp. 365–398.

Mohriak, W.U., Fainstein, R., 2012. Phanerozoic regional geology of the eastern Brazilian margin. In: Roberts, D.G., Bally, A.W. (Eds.), Regional Geology and Tectonics: Phanerozoic Passive Margins, Cratonic Basins and Global Tectonic Maps. Elsevier, Boston, pp. 222–282.
Mohriak, W.U., Rosendahl, B.R., Turner, J.P., Valente, S.C., 2002. Crustal architecture of South Atlantic volcanic margins. Geol. Soc. Am. Spec. Paper 362, 159–202.
Mohriak, W.U., Szatmari, P., Anjos, S., 2012. Salt: geology and tectonics of selected Brazilian basins in their global context. Geol. Soc. Lond. Spec. Publ. 363 (1), 131–158.
Moraes, M.A.S., Blaskovski, P.R., Paraizo, P.L.B., 2006. Architecture of deep-water reservoirs; Arquitetura de reservatorios de aguas profundas. Boletim de Geociencias Da Petrobras, 14 (in Portuguese).
Moraes, L.C., Seer, H.J., 2018. Pillow lavas and fluvio-lacustrine deposits in the northeast of Paraná Continental Magmatic Province, Brazil. J. Volcanol. Geotherm. Res. 355, 78–86. https://doi.org/10.1016/j.jvolgeores.2017.03.024.
Morais Neto, J.M., Hegarty, K.A., Karner, G.D., Alkmim, F.F., 2009. Timing and mechanisms for the generation and modification of the anomalous topography of the Borborema Province, northeastern Brazil. Mar. Pet. Geol. 26, 1070–1086. https://doi.org/10.1016/j.marpetgeo.2008.07.002.
Morgan, W.J., 1983. Hot spot tracks and the early rifting of the Atlantic. Tectonophys 94, 123–139.
Nascimento, I., de Figueiredo, J.P., Azambuja Filho, N.C., Oliveira, J.P., Araújo, A.C., Ferro, R., Borghi, L., 2020. High resolution stratigraphy of channelized deposits on a continental slope setting with sea-floor topography controlled by halokinetics, uppermost Cretaceous, Espírito Santo offshore basin, Brazil. J. South Am. Earth Sci. 103, 102721. https://doi.org/10.1016/j.jsames.2020.102721.
Nemčok, M., 2016. Rifts and Passive Margins: Structural Architecture, Thermal Regimes, and Petroleum Systems. Cambridge University Press.
Noce, C.M., Pedrosa-Soares, A.C., Silva, L.C., Armstrong, R., Piuzana, D., 2007. Evolution of the polycyclic basement complexes in the Araçuaí orogen, based on U-Pb SHRIMP data: Implications for Brazil-Africa links in Paleoproterozoic time. Precambr. Res. 159, 60–78.
Novo, T., Fonte-Boa, T., Rolim, J., Fonseca, A.C., 2021. The state of the art of Low-temperature Thermochronology in Brazil. J. Geol. Surv. Brazil 4, 239–256. https://doi.org/10.29396/jgsb.2021.v4.n3.4.
Ohm, S.E., Karlsen, D.A., Austin, T.J.F., 2008. Geochemically driven exploration models in uplifted areas: examples from the Norwegian Barents Sea. AAPG Bull. 92 (9), 1191–1223.
Oliver, M.A., Webster, R., 2015. Basic Steps in Geostatistics: the Variogram and Kriging. Switzerland, Springer International Publishing, Cham.
Pedrosa-Soares, A. C., Deluca, C., Araujo, C. S., Gradim, C., Lana, C. de C., Dussin, I., Silva, L. C., Babinski, M., 2020. O Orógeno Araçuaí à luz da geocronologia: um tributo a Umberto Cordani, in: Geocronologia e evolução tectônica do Continente Sul-Americano: a contribuição de Umberto Giuseppe Cordani. São Paulo, Solaris Edições Culturais, pp. 250-272 (in Portuguese).
Pedrosa-Soares, A., Noce, C., Wiedemann, C.M., Pinto, C.P., 2001. The Araçuaí-West-Congo Orogen in Brazil: an overview of a confined orogen formed during Gondwanaland assembly. Precambrian Res. 110, 307–323. https://doi.org/10.1016/S0301-9268(01)00174-7.
Pedrosa-Soares, A.C., Noce, C.M., Alkmim, F.F.d., Silva, L.C.d., Babinski, M., Cordani, U., Castañeda, C., 2007. Orógeno Araçuaí: síntese do conhecimento 30 anos após Almeida 1977. Geonomos 15, 1–16 (in Portuguese).
Pedrosa-Soares, A.C., Alkmim, F.F., Tack, L., Noce, C.M., Babinski, M., Silva, L.C., Martins-Neto, M.A., 2008. Similarities and differences between the Brazilian and African counterparts of the Neoproterozoic Araçuaí-West Congo orogen. Geol. Soc. Lond. Spec. Publ. 294 (1), 153–172. https://doi.org/10.1144/SP294.9.
Pedrosa-Soares, A.C., Babinski, M., Noce, C.M., Martins, M., Queiroga, G., Vilela, F., 2011. The Neoproterozoic Macaúbas Group, Araçuaí orogen, SE Brazil. Geol. Soc. Lond. Mem. 36, 523–534.
Pedrosa-Soares, 1997. A geologia da Folha Araçuaí, Minas Gerais. IGC/UFMG, Projeto Espinhaço. Available in: http://www.portalgeologia.com.br/index.php/mapa (in Portuguese).
Peixoto, E., Pedrosa-Soares, A.C., Alkmim, F.F., Dussin, I.A., 2015. A suture–related accretionary wedge formed in the Neoproterozoic Araçuaí orogen (SE Brazil) during Western Gondwanaland assembly. Gondwana Res. 27 (2), 878–896.
Peixoto, E., de Alkmim, F.F., Pedrosa-Soares, A.C., 2018. The Rio Pardo salient, northern Araçuaí orogen: An example of a complex basin-controlled fold-thrust belt curve. Brazilian J. Geol. 48, 25–49. https://doi.org/10.1590/2317-4889201820170134.
Reis, H.L.S., Alkmim, F.F., Fonseca, R.C.S., Nascimento, T.C., Suss, J.F., Prevatti, L.D., 2017. The São Francisco Basin. In: Heilbron, M., Cordani, U.G., Alkmim, F.F. (Eds.), São Francisco Craton. Springer, Eastern Brazil, pp. 117–143. https://doi.org/10.1007/978-3-319-01715-0.
Reuber, K., Mann, P., 2019. Control of Precambrian-to-Paleozoic orogenic trends on along-strike variations in Early Cretaceous continental rifts of the South Atlantic Ocean. Interpretation 7, SH45–SH69. https://doi.org/10.1190/int-2018-0257.1.
Rezende, É.A., Salgado, A.A.R., 2011. Mapeamento de unidades de relevo na média Serra do Espinhaço Meridional-MG. GEOUSP Espaço e Tempo 15 (3), 45–60 (in Portuguese).
Rodovalho, N., Gontijo, R.C., Santos, C.F., Milhomem, P.S., 2007. Bacia de Cumuruxatiba. Boletim de Geociências da Petrobras 15 (2), 485–491 (in Portuguese).
Rouby, D., Braun, J., Robin, C., Dauteuil, O., Deschamps, F., 2013. Long-term stratigraphic evolution of Atlantic-type passive margins: A numerical approach of interactions between surface processes, flexural isostasy and 3D thermal subsidence. Tectonophysics 604, 83–103. https://doi.org/10.1016/j.tecto.2013.02.003.
Saadi, A., 1995. a Geomorfologia Da Serra Do Espinhaço Em Minas Gerais E De Suas Margens in Portuguese Geonomos 3, 41–63. https://doi.org/10.18285/geonomos.v3i1.215.
Sacek, V., 2017. Post-rift influence of small-scale convection on the landscape evolution at divergent continental margins. Earth Planet. Sci. Lett. 459, 48–57. https://doi.org/10.1016/j.epsl.2016.11.026.
Sahu, H.S., Raab, M.J., Kohn, B.P., Gleadow, A.J.W., Kumar, D., 2013. Denudation history of Eastern Indian peninsula from apatite fission track analysis: Linking possible plume-related uplift and the sedimentary record. Tectonophysics 608, 1413–1428. https://doi.org/10.1016/j.tecto.2013.06.002.
Salomon, E., Passchier, C., Koehn, D., 2017. Asymmetric continental deformation during South Atlantic rifting along southern Brazil and Namibia. Gondwana Res. 51, 170–176. https://doi.org/10.1016/j.gr.2017.08.001.
Santiago, R., Caxito, F., Aparecida Neves, M., Dantas, E., de Medeiros, B., Júnior, E., Nascimento Queiroga, G., 2020. Two generations of mafic dyke swarms in the southeastern Brazilian coast: reactivation of structural lineaments during the gravitational collapse of the Araçuaí-Ribeira orogen (500 Ma) and west Gondwana breakup (140 Ma). Precambrian Res. 105344. https://doi.org/10.1016/j.precamres.2019.105344.
Santos, R.F., Alkmim, F.F., Pedrosa-Soares, A.C., 2009. A Formação Salinas, Orógeno Aracuaí (MG): história deformacional e significado tectônico.Revista. Brasileira de Geociências 39 (1), 81–100 (in Portuguese).
Santos, M.N., Chemale, F., Dussin, I.A., Martins, M.S., Queiroga, G., Pinto, R.T.R., Santos, A.N., Armstrong, R., 2015. Provenance and paleogeographic reconstruction of a Mesoproterozoic intracratonic sag basin (Upper Espinhaço Basin, Brazil). Sediment. Geol. 318, 40–57. https://doi.org/10.1016/j.sedgeo.2014.12.006.
Santos, C.F., Cupertino, J.A., Braga, J.A.E., 1990. Síntese sobre a geologia das bacias do Recôncavo, Tucano e Jatobá. In: Raja Gabaglia, G.P., Milani, E.J. (Eds.), Origem e evolução das bacias sedimentares. PETROBRAS, Rio de Janeiro, pp. 235–266 (in Portuguese).
Scherer, C.M.S., 2000. Eolian dunes of the Botucatu Formation (Cretaceous) in Southernmost Brazil: morphology and origin. Sediment. Geol. 137, 63–84. https://doi.org/10.1016/S0037-0738(00)00135-4.
Scherer, C.M.S., Goldberg, K., 2007. Palaeowind patterns during the latest Jurassic-earliest Cretaceous in Gondwana: evidence from aeolian cross-strata of the Botucatu Formation, Brazil. Palaeogeog. Palaeoclimatol. Palaeoecol. 250 (1–4), 89–100. https://doi.org/10.1016/j.palaeo.2007.02.018.
Scherer, C.M.S., Lavina, E.L.C., 2006. Stratigraphic evolution of a fluvial-eolian succession: the example of the Upper Jurassic-Lower Cretaceous Guara and Botucatu formations, Parana Basin, Southernmost Brazil. Gondwana Res. 9, 475–484.
Scherer, C.M.S., Lavina, E.L.C., Dias Filho, D.C., Oliveira, F.M., Bongiolo, D.E., Aguiar, E. S., 2007. Stratigraphy and facies architecture of the fluvial-aeolian-lacustrine Sergi Formation (Upper Jurassic), Recôncavo Basin, Brazil. Sediment. Geol. 194, 169–193. https://doi.org/10.1016/j.sedgeo.2006.06.002.
Silva, D.R., Mizusaki, A.M.P., Milani, E.J., Pimentel, M., 2012. Depositional ages of Paleozoic and Mesozoic pre-rift supersequences of the Recôncavo Basin in northeastern Brazil: A Rb-Sr radiometric study of sedimentary rocks. J. South Am. Earth Sci. 37, 13–24. https://doi.org/10.1016/j.jsames.2011.12.006.
Silva, D., Piazolo, S., Daczko, N.R., Houseman, G., Raimondo, T., Evans, L., 2018. Intracontinental orogeny enhanced by far-field extension and local weak crust. Tectonics 37 (12), 4421–4443. https://doi.org/10.1029/2018TC005106.
Sloss, L.L., Speed, R.C., 1974. Relationships of cratonic and continental-margin tectonic episodes. Soc. Econ. Paleontol. Mineral Spec. Publ. 22, 98–119.
Sloss, L.L., 1988. Introduction. In: Sloss, L.L. (Ed.), Sedimentary Cover—North American Craton. The Geology of North America, DI. Geological Society of America, Boulder, CO, 1–3.
Sobreira, J.F.F., Szatmari, P., 2003. Idades Ar-Ar para as rochas ígneas do arquipélago de Abrolhos, margem sul da Bahia. In: Simpósio Nacional de Estudos Tectônicos, 9.; International Symposium on Tectonics, 3., Búzios, Rio de Janeiro. Boletim de Resumos, Rio de Janeiro, pp. 382–383 (in Portuguese).
Sobreira, J.F.F., França, R.L., 2006. Um modelo tectono-magmático alternativo para a região do Complexo Vulcânico de Abrolhos. Boletim de Geociências da Petrobras 14 (1), 143–147 (in Portuguese).
Souza, D.H., Hackspacher, P.C., Silva, B.V., Siqueira-Ribeiro, M.C., Hiruma, S.T., 2021. Temporal and spatial denudation trends in the continental margin of southeastern Brazil. J. South Am. Earth Sci. 105, 102931. https://doi.org/10.1016/j.jsames.2020.102931.
Stanley, J.R., Braun, J., Baby, G., Guillocheau, F., Robin, C., Flowers, R.M., Brown, R., Wildman, M., Beucher, R., 2021. Constraining plateau uplift in Southern Africa by combining thermochronology, sediment flux, topography, and landscape evolution modeling. J. Geophys. Res. Solid Earth 126, 1–34. https://doi.org/10.1029/2020jb021243.
Stanton, N., Gordon, A.C., Valente, S.C., Mohriak, W.U., Maia, T.M., Arena, M., 2022. The Abrolhos Magmatic Province, the largest postbreakup magmatism of the Eastern Brazilian margin: a geological, geophysical, and geochemical review. In: Santos, A.C., Hackspacher, P.C. (Eds.), Meso-Cenozoic Brazilian Offshore Magmatism: Geochemistry, Petrology and Tectonics. Elsevier Inc., pp. 189–230. https://doi.org/10.1016/B978-0-12-823988-9.00014-9.
Strozyk, F., Back, S., Kukla, P.A., 2017. Comparison of the rift and post-rift architecture of conjugated salt and salt-free basins offshore Brazil and Angola/Namibia, South Atlantic. Tectonophysics 716, 204–224. https://doi.org/10.1016/j.tecto.2016.12.012.

Summerfield, M.A., 1991. Global Geomorphology. Longman.
Tack, L., Wingate, M.T.D., Liégeois, J.P., Fernandez-Alonso, M., Deblond, A., 2001. Early Neoproterozoic magmatism (1000–910 Ma) of the Zadinian and Mayumbian groups (Bas-Congo): onset of Rodinia rifting at the western edge of the Congo craton. Precambrian Res. 110, 277–306. https://doi.org/10.1016/S0301-9268(01)00192-9.
Tedeschi, M., Novo, T., Pedrosa-Soares, A., Dussin, I., Tassinari, C., Silva, L.C., Gonçalves, L., Alkmim, F., Lana, C., Figueiredo, C., Dantas, E., Medeiros, S., De Campos, C., Corrales, F., Heilbron, M., 2016. The Ediacaran Rio Doce magmatic arc revisited (Araçuaí-Ribeira orogenic system, SE Brazil). J. South Am. Earth Sci. 68, 167–186. https://doi.org/10.1016/j.jsames.2015.11.011.
Temporim, F.A., Bellon, U.D., Domeier, M., Trindade, R.I.F.D., D'Agrella-Filho, M.S., Tohver, E., 2021. Constraining the Cambrian drift of Gondwana with new paleomagnetic data from post-collisional plutons of the Araçuaí orogen, SE Brazil. Precambrian Res. 359, 106212. https://doi.org/10.1016/j.precamres.2021.106212.
Thomaz Filho, A., de Cesaro, P., Mizusaki, A.M.P., Leão, J.G., 2005. Hot spot volcanic tracks and their implications for South American plate motion, Campos Basin (Rio de Janeiro state). Brazil. J. South Am. Earth Sci. 18, 383–389. https://doi.org/10.1016/j.jsames.2004.11.006.
Tohver, E., D'Agrella-Filho, M.S., Trindade, R.I.F., 2006. Paleomagnetic record of Africa and South America for the 1200–500 Ma interval, and evaluation of Rodinia and Gondwana assemblies. Precambrian Res. 147, 193–222. https://doi.org/10.1016/j.precamres.2006.01.015.
Torsvik, T.H., Rousse, S., Labails, C., Smethurst, M.A., 2009. A new scheme for the opening of the South Atlantic Ocean and the dissection of an Aptian salt basin. Geophys. J. Int. 177, 1315–1333. https://doi.org/10.1111/j.1365-246X.2009.04137.x.
Trompette, R., 1994. Geology of Western Gondwana (500 Ma). Balkema, Amsterdam, p. 350.
Trompette, R., Silva, M., Tomassi, A., Vauchez, A., Uhlein, A., 1993. Western Gondwana's agglutination during the Pan- African/Brasiliano Cycle and the role of the geometry of the São Francisco Craton in the architecture of the Ribeira fold Belt. Rev. Bras. Geoc. 23, 193–287.
Valadão, R.C., 2009. Geodinâmica de superfícies de aplanamento, desnudação continental e tectônica ativa como condicionantes da megageomorfologia do Brasil Oriental. Rev Brasil Geomorfol 10 (2), 77–90 (in Portuguese).
Van Ranst, G., Pedrosa-Soares, A.C., Novo, T., Vermeesch, P., De Grave, J., 2020a. New insights from low-temperature thermochronology into the tectonic and geomorphologic evolution of the south-eastern Brazilian highlands and passive margin. Geosci. Front. 11, 303–324. https://doi.org/10.1016/j.gsf.2019.05.011.
Van Ranst, G., Baert, P., Fernandes, A.C., De Grave, J., 2020b. Technical note: Nikon–TRACK *Flow*, a new versatile microscope system for fission track analysis. Geochronology 2, 93–99. https://doi.org/10.5194/gchron-2-93-2020.
Van Ranst, G., Fonseca, A.C., Tack, L., Delvaux, D., Baudet, D., Kitambala, N.Y., Pay, A. L., De Grave, J., 2022. Exhumation of the passive margin of the DR Congo during pre- and post- Gondwana breakup: evidence from low-temperature thermochronology, geology and geomorphology. Geomorphology 398, 108067. https://doi.org/10.1016/j.geomorph.2021.108067.
Vaughan, A.P.M., Pankhurst, R.J., 2008. Tectonic overview of the West Gondwana margin. Gondwana Res. 13, 150–162. https://doi.org/10.1016/j.gr.2007.07.004.
Vermeesch, P., 2018. IsoplotR: A free and open toolbox for geochronology. Geosci. Front. 9, 1479–1493. https://doi.org/10.1016/j.gsf.2018.04.001.
Vieira, R.A.B., Mendes, M.P., Vieira, P.E., Costa, L.A.R., Tagliari, C.V., Bacelar, L.A.P., Feijó, F.J., 1994. Bacias do Espírito Santo e Mucuri. Bol. Geociências Petrobras 8 (1), 191–202 (in Portuguese).
Vilela, F.T., Pedrosa-Soares, A., Babinski, M., Lana, C., Trindade, R.I.F., Santos, E., 2021. Diamictitic iron formation (DIF) deposits of the Neoproterozoic Nova Aurora Iron District (Macaúbas Group, Southeast Brazil). J. South Am. Earth Sci. 112, 103614. https://doi.org/10.1016/j.jsames.2021.103614.
Wagner, G.A., van den Haute, P., 1992. Fission Track Dating. Kluwer Academic Publishers, Dordrecht.
Wildman, M., Cogné, N., Beucher, R., 2019. Fission-track thermochronology applied to the evolution of passive continental margins. In: Malusà, M., Fitzgerald, P. (Eds.), Fission-track Thermochronology and Its Application to Geology. Springer Textbooks in Earth Sciences, Geography and Environment. Springer, Cham. https://doi.org/10.1007/978-3-319-89421-8_20.
Zalán, P.V., 2005. Evolução fanerozóica das bacias sedimentares brasileiras. Geologia do Continente Sul-Americano: evolução da obra de Fernando Flávio Marques de Almeida. São Paulo, Beca, pp. 595–613 (in Portuguese).
Zhang, Q., Alves, T.M., Martins-Ferreira, M.A.C., 2022. Fault analysis of a salt minibasin offshore Espírito Santo, SE Brazil: implications for fluid flow, carbon and energy storage in regions dominated by salt tectonics. Mar. Pet. Geol. 143, 105805. https://doi.org/10.1016/j.marpetgeo.2022.105805.
Henry, S.G., Mohriak, W.U., Mello, M.R., 1996. South Atlantic sag basins: new petroleum system components. AAPG International Conference and Exhibition, Caracas, Venezuela. Abstract in: American Association of Petroleum Geologists Bulletin, vol. 80/8, p. 1300.